Dynamical Analysis of a Melanoma Model with Immune Response

Article *in* International Journal of Bifurcation and Chaos · July 2022

DOI: 10.1142/S0218127422501292

3 authors, including:

Daifeng Duan
Nanjing University of Posts and Telecommunications
11 PUBLICATIONS **125** CITATIONS

SEE PROFILE

International Journal of Bifurcation and Chaos, Vol. 32, No. 9 (2022) 2250129 (28 pages)

DOI: 10.1142/S0218127422501292

Dynamical Analysis of a Melanoma Model with Immune Response

Qinrui Dai, Daifeng Duan and Yuxiao Guo*
Department of Mathematics,
Harbin Institute of Technology,
Weihai 264209, P. R. China
**gyx@hit.edu.cn*

Received July 26, 2021; Revised January 4, 2022

In this paper, we study the stability and bifurcation behavior of a three-dimensional melanoma model with immune response. The system has at least one and at most three positive equilibria. It is proved that the system undergoes Hopf bifurcation and saddle-node bifurcation at the positive equilibrium. We investigate the direction of Hopf bifurcation and stability of the bifurcating periodic solution by center manifold theorem and normal form theory. Moreover, codimension two bifurcations of the system are analyzed. We demonstrate the existence of Bautin bifurcation and Bogdanov–Takens bifurcation of the system. The normal form of Bautin bifurcation and Bogdanov–Takens bifurcation are given. Finally, some numerical simulations are demonstrated to support our theoretical results, and the importance of some parameters of the system is discussed, in particular the activation rate of CD8+T cells.

Keywords: Melanoma model; immune response; Hopf bifurcation; Bautin bifurcation; Bogdanov–Takens bifurcation.

1. Introduction

Melanoma is a kind of skin cancer with a high mortality rate, and its early detection is very sophisticated [Friedman *et al.*, 1985; Terushkin & Halpern, 2009]. It has gradually become a global disease, and the number of cases is increasing year by year [Karimkhani *et al.*, 2017; Villani *et al.*, 2020]. There are complex interactions between melanoma cells and the immune system in patients, which renders the reasoning of treatment difficult [Bromley *et al.*, 2001; d'Onofrio, 2005; Hu *et al.*, 2020]. Now, many scholars have established mathematical models to study the tumor-immune. For example, Makhlouf *et al.* [2020] studied the role of CD4+T cells in tumor-immune through stability and bifurcation methods. Wang *et al.* [2020] established a two-dimensional tumor-immune model with nonlinear functional response and diffusion, and analyzed the effect of diffusion on the existence of nonconstant positive steady states and the steady-state bifurcations. Alvarez *et al.* [2019] discussed cell-mediated immune response for intra-tumor heterogeneity by learning a nonlinear mathematical model. Recently, immune checkpoint proteins and immune checkpoint inhibitors have played an important role in cancer treatment [Agur *et al.*, 2016; Lim *et al.*, 2017; Hargadon *et al.*, 2018], including melanoma, which makes the mathematical model of melanoma based on immunotherapy further developed.

*Author for correspondence

Tsur *et al.* [2020] established a mathematical model of immune response among antigen-presenting cells, melanoma cells and CD8+T cells

$$\begin{cases} \dfrac{dA}{dt} = \alpha_A \dfrac{M}{M+b} - \mu_A A, \\ \dfrac{dT}{dt} = \alpha_e A - \mu_e T, \\ \dfrac{dM}{dt} = \gamma_{\text{mel}} M - \upsilon_{\text{mel}} \dfrac{TM}{M+g}, \end{cases} \tag{1}$$

where t is the time, A, T, and M are the number of antigen-presenting cells, CD8+T cells, and melanoma cells in patients with melanoma at time t, respectively. The parameters α_A, b, and μ_A stand for the activation rate, the semi-saturation coefficient and the mortality rate of antigen-presenting cells, respectively. α_e and μ_e denote the activation rate of antigen-presenting cells to CD8+T cells and the apoptosis rate of CD8+T cells, respectively. γ_{mel}, υ_{mel} and g represent the proliferation rate of melanoma cells, the clearance rate of CD8+T cells to melanoma cells, and the semi-saturation constant of melanoma cells, respectively. Multiple steady states and the stability of this system were discussed. However, many researchers [Li *et al.*, 2015; Ashyani *et al.*, 2018; Yu & Jang, 2019] believe that tumor cells exist with the maximum carrying capacity in the human body. Thus, we consider the effect of carrying capacity on the model given in [Tsur *et al.*, 2020], which is described by the following model of three-dimensional differential equation

$$\begin{cases} \dfrac{dA}{dt} = \alpha_A \dfrac{M}{M+b} - \mu_A A, \\ \dfrac{dT}{dt} = \alpha_e A - \mu_e T, \\ \dfrac{dM}{dt} = \gamma_{\text{mel}} M \left(1 - \dfrac{M}{k}\right) - \upsilon_{\text{mel}} \dfrac{TM}{M+g}, \end{cases} \tag{2}$$

where the maximum size which melanoma can occupy is limited by carrying capacity k. Many literatures have explained the maximum capacity of tumor cells. Generally, the capacity of human individual resources, medical treatment and patients' life attitude play a blocking role in the growth of melanoma, and with the increase of the number of tumor cells, the blocking effect becomes greater and greater. Thus, the blocking growth model is more in line with the growth law of melanoma. More specifically, in Eq. (2), $\gamma_{\text{mel}} M$ reflects the growth trend of melanoma itself, while $(1 - \frac{M}{k})$ shows the blocking effect of environment and resources on the growth of melanoma.

In this paper, the dynamic analysis of a melanoma model with immune response is investigated. The dynamic properties of system (2) are mainly studied from the perspectives of equilibrium stability, Hopf bifurcation, Bogdanov–Takens bifurcation and Bautin bifurcation. First, the nonnegativity and boundedness of the solution of the given system are proved. The bifurcation diagram of the system is done with the parameters of α_e and g. On this basis, the existence, stability and codimension one bifurcations of positive equilibrium are studied. It is proved that the system undergoes Hopf bifurcation and saddle-node bifurcation at the positive equilibrium, and the properties of Hopf bifurcation under different parameters are given. Second, the codimension two bifurcations of the system are analyzed. We discuss the existence of Bautin bifurcation and Bogdanov–Takens bifurcation of the positive equilibrium. By center manifold theorem and normal form theory, we calculate the normal form and homoclinic orbit expression of Bogdanov–Takens bifurcation. Finally, different parameters are selected to simulate the theoretical results. The simulation results of Hopf bifurcating periodic solution are obtained by fixing parameters and constant changes, and with the appearance of Bogdanov–Takens bifurcation homoclinic orbit, the periodic solution will disappear. For the Bautin bifurcation, the existence and asymptotic stability of different periodic solutions are obtained by taking values near the Bautin point. There are two innovations in this paper: (i) introducing the maximum carrying capacity of melanoma cells to make the model more in line with the actual biological significance and the dynamical properties of the model are then studied from the point of view of codimension one and codimension two bifurcations respectively. (ii) It is found that there are complex dynamical phenomena, such as homoclinic orbits and multistability coexisting in the two-parameter plane. Model (2) is a relatively new melanoma model, and the research on the dynamic properties of this model has not been well developed. Codimension two bifurcations are usually accompanied by abundant dynamic phenomena, especially when there are multiple codimension two bifurcations in a model. Therefore, this

paper focuses on some interesting dynamic phenomena of model (2) from the perspective of high codimension bifurcations, which is the main innovation of this paper.

The rest of this paper is organized as follows. In Sec. 2, we analyze the boundedness and stability of solutions to system (2) and the two-parameter bifurcation diagram is also given in this section. Codimension one bifurcations are investigated in Sec. 3, and we first obtain the existence of saddle-node bifurcation and Hopf bifurcation at the positive equilibrium. Then, we investigate the direction of Hopf bifurcation and stability of the bifurcating periodic solution by center manifold theorem and normal form theory. We study the codimension two Bogdanov–Takens bifurcation and Bautin bifurcation in Sec. 4 and the normal form of bifurcations are given. In order to support our theoretical analysis, given the bifurcation diagram, in Sec. 2, we give some numerical simulations for different parameters in Sec. 5. Finally, a brief conclusion and discussion section complete the paper.

2. Boundedness and Stability

In this section, we mainly discuss the boundedness of any non-negative solution, the existence and the local stability of positive equilibrium to system (2). Then, in order to better illustrate the abundant dynamic phenomena of the model, we give the bifurcation diagram of the system with two parameters in advance.

2.1. *Non-negativity and boundedness of solution*

The right-hand side function of system (2) is continuous on $\mathbb{R}^3_+$ and satisfies the Lipschitz condition concerning A, T, and M. Therefore, the system has a unique solution. Then, we consider the non-negativity and boundedness of the solution.

Theorem 1. *All solutions of system (2) initiating in $\mathbb{R}^3_+$ are non-negative and are attracted to K, where*

$$K = \left\{(A,T,M) \in \mathbb{R}^3_+ : \right.$$
$$\left. 0 \le A \le \frac{\alpha_A}{\mu_A}, 0 \le T \le \frac{\alpha_e \alpha_A}{\mu_e \mu_A}, 0 \le M \le k \right\}.$$

Proof. It is clear that for system (2), the solution with a non-negative initial value is still non-negative, that is $\mathbb{R}^3_+$ invariant. Thus, we only prove the boundedness of the solution. From system (2), we have

$$\begin{cases} -\mu_A A \le \dfrac{dA}{dt} \le \alpha_A - \mu_A A, \\ -\mu_e T \le \dfrac{dT}{dt} \le \alpha_e A - \mu_e T, \\ -\upsilon_{\text{mel}} TM \le \dfrac{dM}{dt} \le \gamma_{\text{mel}} M\left(1 - \dfrac{M}{k}\right). \end{cases} \tag{3}$$

From the first inequality in (3), the following equations are considered:

$$\frac{\mathrm{d}x}{\mathrm{d}t} = -\mu_A x, \quad \frac{\mathrm{d}y}{\mathrm{d}t} = \alpha_A - \mu_A y \tag{4}$$

and we then have

$$x = x(t_0)e^{-\mu_A t} \ge 0, \quad y = \frac{\alpha_A}{\mu_A} - \frac{y(t_0)}{\mu_A} e^{\mu_A t} \le \frac{\alpha_A}{\mu_A}.$$

According to the comparison theorem of ordinary differential equation, we can see that when the initial value of $A(t)$ is the same as that of equations $\frac{\mathrm{d}x}{\mathrm{d}t} = -\mu_A x$ and $\frac{\mathrm{d}y}{\mathrm{d}t} = \alpha_A - \mu_A y$, then $0 \le A(t) \le \frac{\alpha_A}{\mu_A}$. Moreover, if the condition $A(t_0) \in [0, \frac{\alpha_A}{\mu_A}]$ is satisfied, then $A(t) \in [0, \frac{\alpha_A}{\mu_A}]$. In the same way, from the second and third inequalities of (3), we can get $0 \le T \le \frac{\alpha_e \alpha_A}{\mu_e \mu_A}$ and $0 \le M \le k$. Thus, the boundedness of the system (2) is proved. ■

After introducing the maximum capacity k into model (1), there are complex dynamical phenomena, such as homoclinic orbits and multistability coexisting in the two-parameter plane, which is not found in the original model (1). Many similar tumor models [Yu *et al.*, 2017; Zeng & Ma, 2020] give the parameter selection of numerical simulations. After analysis, by selecting parameters α_e and g as bifurcation parameters, and the other parameter values selected, we get as follows

$$\alpha_A = 1, \quad b = 0.42, \quad \mu_A = 0.1, \quad \mu_e = 0.5,$$
$$\gamma_{\text{mel}} = 0.31519, \quad \upsilon_{\text{mel}} = 0.6, \quad k = 10.$$

The main purpose of selecting these parameters is to simulate the abundant codimension two bifurcations of the system (2) in an effective way, such as two-parameter bifurcation diagram, so as to

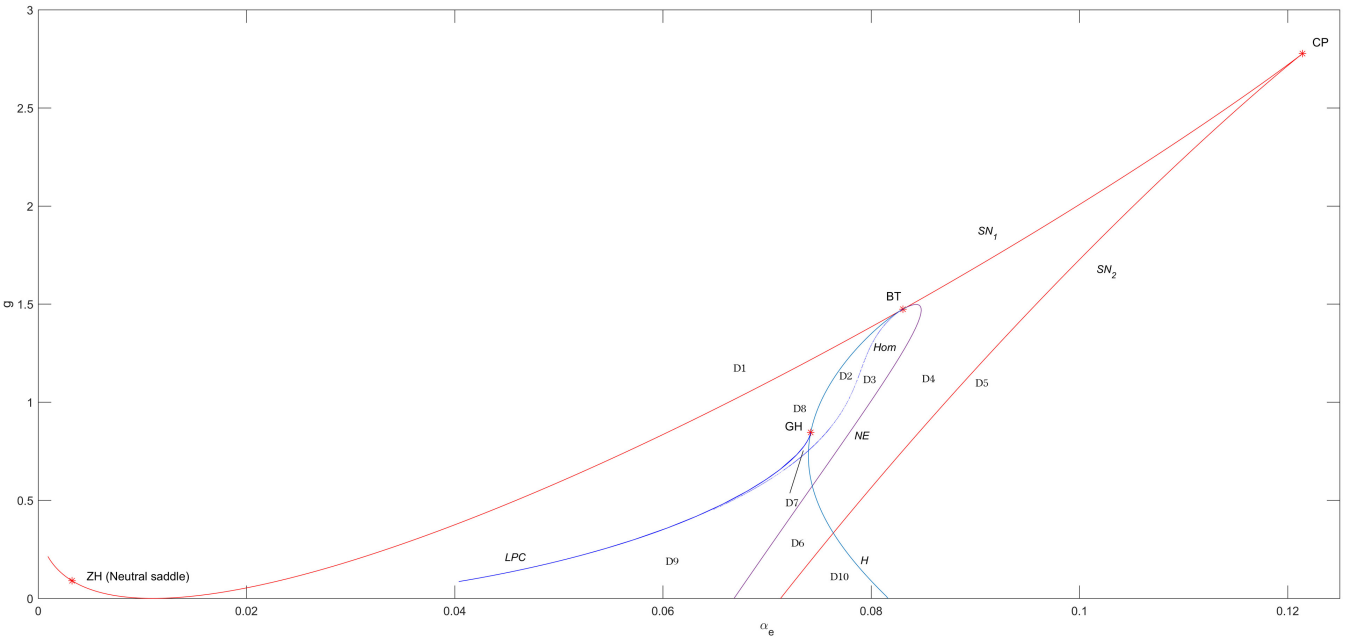

Fig. 1. Bifurcation diagram of system (2) in (α_e–g)-plane. The meaning of the curves are as follows: H (light blue) Hopf; SN (red) saddle-node; LPC (dark blue) limit point of cycles; Hom (blue dotted) homoclinic; NE (purple) neutral saddle equilibrium. Special points are BT (Bogdanov–Takens), GH (Bautin) and CP (Cusp point), ZH (Zero-Hopf). D1–D10 represent the label of different regions.

illustrate some interesting dynamic phenomena of the system and to see some results which are reasonable from the biological point of view. The bifurcation diagram of system (2) in (α_e–g)-plane can be obtained, as shown in Fig. 1.

From Fig. 1, it can be observed that saddle-node bifurcation curve (SN_1) and Hopf bifurcation curve are tangent at $(\alpha_e, g) = (0.083051, 1.474154)$, and the tangent point corresponds to BT point of Fig. 1, which indicates that system (2) undergoes Bogdanov–Takens bifurcation at this point. System (2) exists Bautin bifurcation at the lower left Hopf bifurcation curve of BT point, corresponding to GH point of Fig. 1. In the saddle-node bifurcation curve, there is a Cusp point bifurcation and a Zero-Hopf point (unfortunately, it is a neutral saddle point and the Zero-Hopf bifurcation is not found in the positive parameter plane), labeled CP and ZH in Fig. 1, respectively. Moreover, three positive equilibria are corresponding to E_2, E_3, and E_4 in the sharp region surrounded by two saddle-node bifurcations, where E_2 and E_4 are stable and E_3 is unstable. On the left saddle-node bifurcation curve, E_2 and E_3 will collide into E_2^*, and on the right saddle-node bifurcation curve, E_3 and E_4 will collide into E_4^*. There is a unique positive equilibrium E_1 outside this sharp region, which is stable.

In the following parts of the paper, we will introduce the existence and stability of equilibrium points, codimension one bifurcations and codimension two bifurcations based on Fig. 1.

2.1.1. *Existence and stability of positive equilibrium*

As we all know, $E_0 = (0, 0, 0)$ is a zero equilibrium of system (2), and the Jacobian matrix of this equilibrium point is

$$J_{E_0} = \begin{pmatrix} -\mu_A & 0 & \dfrac{\alpha_A}{b} \\ \alpha_e & -\mu_e & 0 \\ 0 & 0 & \gamma_{\text{mel}} \end{pmatrix}.$$

The characteristic equation of this matrix is

$$(\lambda + \mu_A)(\lambda + \mu_e)(\lambda - \gamma_{\text{mel}}) = 0.$$

Therefore, the eigenvalues of this matrix are $-\mu_A$, $-\mu_e$, γ_{mel}, and the boundary equilibrium E_0 is unstable due to $\gamma_{\text{mel}} > 0$. There is no boundary equilibrium in system (2). Next, we prove the existence of positive equilibrium of system (2). Suppose that $E^* = (A^*, T^*, M^*)$ is a positive equilibrium of system (2) with A^*, T^*, $M^* > 0$, then (A^*, T^*, M^*)

must satisfy

$$\begin{cases} \alpha_A \dfrac{M^*}{M^*+b} - \mu_A A^* = 0, \\ \alpha_e A^* - \mu_e T^* = 0, \\ \gamma_{\text{mel}} M^* \left(1 - \dfrac{M^*}{k}\right) - \upsilon_{\text{mel}} \dfrac{T^* M^*}{M^*+g} = 0. \end{cases} \tag{5}$$

From Eq. (5), we have

$$(M^*+b)(M^*+g)(M^*-k) + \tilde{k}M^* = 0, \tag{6}$$

where

$$\tilde{k} = k\frac{\upsilon_{\text{mel}}\alpha_A\alpha_e}{\gamma_{\text{mel}}\mu_A\mu_e}.$$

We define the function

$$P(M^*) = (M^*+b)(M^*+g)(M^*-k) + \tilde{k}M^*,$$

and study the existence of the zero point of the function $P(M^*)$ in the interval $(0,+\infty)$. The following quadratic equation is gained by deriving Eq. (5) with respect to M^*,

$$P'(M^*) = 3(M^*)^2 + 2(b+g-k)M^* + bg + \tilde{k} - k(b+g). \tag{7}$$

The discriminant of quadratic equation corresponding to (7) is as follows

$$\Delta = 4(b+g-k)^2 - 12[bg + \tilde{k} - k(b+g)].$$

For convenience, the expressions of the two roots of quadratic equation corresponding to (7) are given here

$$\begin{cases} M_c = \dfrac{2(b+g-k) - \sqrt{\Delta}}{6}, \\ M_d = \dfrac{2(b+g-k) + \sqrt{\Delta}}{6}. \end{cases}$$

The following three cases are discussed.

(1) $b+g-k > 0$: the symmetry axis of quadratic equation is on the left side of vertical axis. If there is $bg + \tilde{k} - k(b+g) > 0$, then $P'(M^*) > 0$ holds in the interval $(0,+\infty)$. Thus, the function $P(M^*)$ monotonically increases in $(0,+\infty)$ and due to $P(0) = -kbg < 0$, $P(M^*)$ has a unique zero point in $(0,+\infty)$.

(2) $b+g-k < 0$: the symmetry axis of quadratic equation is on the right side of vertical axis. If there are both $bg + \tilde{k} - k(b+g) > 0$ and $\Delta > 0$, then we have $P'(M^*) > 0$ in $(0, M_c) \cup (M_d, +\infty)$ and $P'(M^*) < 0$ in (M_c, M_d). In this case, $P(M^*)$ monotonically increases in $(0, M_c)$, $(M_d, +\infty)$ and monotonically decreases in (M_c, M_d). Furthermore, if $P(M_c) > 0$ and $P(M_d) < 0$ exist, then $P(M^*)$ has three different zeros in $(0,+\infty)$.

(3) $bg + \tilde{k} - k(b+g) < 0$: In this case, no matter what the sign of $b+g-k$ is, there are $P'(M^*) < 0$ in $(0, M_d)$ and $P'(M^*) > 0$ in $(M_d, +\infty)$. Therefore, $P(M^*)$ monotonically decreases in $(0, M_d)$ and monotonically increases in $(M_d, +\infty)$. $P(M^*)$ has a unique zero in $(0,+\infty)$.

The existence of positive equilibrium of system (2) is summarized in Theorems 2 and 3.

Theorem 2. *For system (2).*

(i) *There is a unique positive equilibrium point* $E_1(A_1, T_1, M_1)$, *when* $b+g-k > 0$, $bg + \tilde{k} - k(b+g) > 0$ *or* $bg + \tilde{k} - k(b+g) < 0$.

(ii) *There are three different positive equilibrium points* $E_2(A_2, T_2, M_2)$, $E_3(A_3, T_3, M_3)$ *and* $E_4(A_4, T_4, M_4)$, *when* $bg + \tilde{k} - k(b+g) > 0$, $\Delta > 0$ *and* $P(M_c) > 0$, $P(M_d) < 0$.

Remark 2.1. In fact, for Theorem 2(ii), if $P(M_c) = 0$ and other conditions remain the same, then the system admits an instantaneous equilibrium $E_2^*(A_2^*, T_2^*, M_2^*)$, formed by the collision of E_2 and E_3. If $P(M_d) = 0$ and other conditions remain unchanged, then the system admits an instantaneous equilibrium $E_4^*(A_4^*, T_4^*, M_4^*)$, formed by the collision of E_3 and E_4.

Theorem 3. *For system (2), there is at least one positive equilibrium.*

Proof. Due to

$$P(0) = -kbg < 0 \quad \text{and} \quad \lim_{M \to +\infty} P(M) = +\infty,$$

there exists $M^* \in (0,+\infty)$ such that $P(M^*) = 0$. Therefore, the function $P(M^*)$ has at least one zero point; That is, the system (2) has at least one positive equilibrium. ■

Next, we study the stability of different positive equilibria. The Jacobian matrix of any positive

equilibria $E_i(A_i, T_i, M_i)$ is

$$J_{E_i} = \begin{pmatrix} -\mu_A & 0 & \alpha_A \dfrac{b}{(M_i+b)^2} \\ \alpha_e & -\mu_e & 0 \\ 0 & -\upsilon_{\mathrm{mel}} \dfrac{M_i}{M_i+g} & \gamma_{\mathrm{mel}} \left(1 - \dfrac{2M_i}{k}\right) - \upsilon_{\mathrm{mel}} \dfrac{T_i g}{(M_i+g)^2} \end{pmatrix}.$$

The characteristic polynomial of Jacobian matrix J_{E_i} is

$$F(\lambda) = (\lambda + \mu_A)(\lambda + \mu_e)(\lambda - \overline{\Delta}_1(E_i)) + \overline{\Delta}_2(E_i),$$

where

$$\begin{aligned} \overline{\Delta}_1(E_i) &= -\upsilon_{\mathrm{mel}} \frac{T_i g}{(M_i+g)^2} + \gamma_{\mathrm{mel}} \left(1 - \frac{2M_i}{k}\right) \\ &= \gamma_{\mathrm{mel}} \left[\left(1 - \frac{2M_i}{k}\right) - \left(1 - \frac{M_i}{k}\right) \frac{g}{M_i+g} \right], \\ \overline{\Delta}_2(E_i) &= \alpha_A \alpha_e \upsilon_{\mathrm{mel}} \frac{b}{(M_i+b)^2} \frac{M_i}{M_i+g} \\ &= \gamma_{\mathrm{mel}} \mu_A \mu_e \left(1 - \frac{M_i}{k}\right) \frac{b}{M_i+b}. \end{aligned}$$

We now have the following theorem, establishing the stability of the nontrivial equilibria.

Theorem 4. *For any positive equilibrium point E_i of system (2), the positive equilibrium is locally asymptotically stable, if (8) holds*

$$\begin{cases} \overline{\Delta}_2(E_i) > \overline{\Delta}_1(E_i)\mu_A\mu_e, \\ \dfrac{dF(\lambda, \overline{\Delta}_2(E_i) = 0)}{d\lambda}\Big|_{\lambda=0} > 0. \end{cases} \tag{8}$$

Proof. When $\overline{\Delta}_2(E_i) = 0$, the roots of the characteristic equation are $-\mu_A$, $-\mu_e$ and $\overline{\Delta}_1(E_i)$, which are all real. When the second inequality of (8) holds, $F(\lambda)$ monotonically increases in $(0, +\infty)$. If $\overline{\Delta}_2(E_i)$ is gradually increased, the function graph of $F(\lambda)$ will shift to the vertical axis, and then the positive root of the characteristic equation will gradually decrease and finally become negative. That is to say, the positive equilibrium is locally asymptotically stable. Let us look for the critical value $\overline{\Delta}_2'(E_i)$ of $\overline{\Delta}_2(E_i)$. When $\overline{\Delta}_1(E_i)$ passes through the origin, we have

$$F(\lambda = 0, \overline{\Delta}_2 = \overline{\Delta}_2') = 0. \tag{9}$$

By substituting (6) into (9), we can get

$$\overline{\Delta}_2'(E_i) = \mu_A \mu_e \overline{\Delta}_1(E_i).$$

Therefore, when $\overline{\Delta}_2(E_i) > \overline{\Delta}_2'(E_i)$, i.e. the first inequality of (8) holds, all the roots of the characteristic equation are negative, and the positive equilibrium E_i of system (2) is locally asymptotically stable. ■

2.2. *Saddle-node and Hopf bifurcation*

In this part, we will analyze codimension one bifurcations of system (2). We first obtain the existence of saddle-node bifurcation and Hopf bifurcation by using the theories in [Shan & Zhu, 2014], and the stability and direction of Hopf bifurcation are elaborated according to the center manifold theorem and the normal form theory [Kuznetsov, 2013].

2.2.1. *Saddle-node bifurcation*

It can be seen from Theorem 2 that when system (2) satisfies the given conditions, there will be three different positive equilibria. Furthermore, if $P(M_c) = 0$ (or $P(M_d) = 0$) is true, the equilibria E_2 (or E_4) and E_3 coalesce, and instantaneous equilibrium E_2^* (or E_4^*) appears. These two instantaneous equilibria will disappear with the emergence of saddle-node bifurcation. The existence condition of the saddle-node bifurcation of system (2) is given by Theorem 5.

Theorem 5. *When $\overline{\Delta}_2 = \overline{\Delta}_1 \mu_A \mu_e$, if there is an instantaneous equilibrium point E_2^* or E_4^*, then the saddle-node bifurcation occurs at E_2^* or E_4^*.*

Proof. For the instantaneous equilibrium point E_2^*, when $\overline{\Delta}_2(E_2^*) = \overline{\Delta}_1(E_2^*)\mu_A\mu_e$, the characteristic polynomial of E_2^* has zero eigenvalue $\lambda_1 = 0$, and we can choose α_e as the bifurcation parameter. Let $\alpha_e = \alpha_e + \varepsilon$. By calculation, the dynamics of the system (2) restricted to the center manifold is determined by

$$\dot{x} = O(\varepsilon^2)x + [s_{11} + (a_2 s_{12} + b_2 s_{13})\varepsilon + O(\varepsilon^2)]x^2 + O(x^3), \tag{10}$$

where $s_{11} > 0$, $s_{12} > 0$, $s_{13} > 0$, $a_2 > 0$, $b_2 > 0$. Denote the right side of system (10) as $F_1(x, \varepsilon)$, and we can get

$$\begin{aligned} &F_1(0,0) = 0,\\ &\frac{\partial F_1}{\partial x}(0,0) = 0, \quad \frac{\partial F_1}{\partial \varepsilon}(0,0) = 0,\\ &\frac{\partial F_1}{\partial x \partial \varepsilon}(0,0) = 2(a_2 s_{12} + b_2 s_{13}),\\ &\frac{\partial^2 F_1}{\partial^2 x}(0,0) = 2s_{11}. \end{aligned}$$

Therefore, when $\overline{\Delta}_2(E_2^*) = \overline{\Delta}_1(E_2^*)\mu_A\mu_e$, the system has saddle-node bifurcation at instantaneous equilibrium E_2^*. Similarly, when $\overline{\Delta}_2(E_4^*) = \overline{\Delta}_1(E_4^*)\mu_A\mu_e$ is appropriate, the system has saddle-node bifurcation at instantaneous equilibrium E_4^*. ■

2.2.2. *Hopf bifurcation*

In this part, we give the existence and the properties of Hopf bifurcation by using the normal form theory based on [Kuznetsov, 2013]. To this end, let us consider the positive equilibrium point E_2 and the corresponding characteristic equation is

$$\begin{aligned} &\lambda^3 + [\mu_A + \mu_e - \overline{\Delta}_1(E_2)]\lambda^2\\ &\quad + [\mu_A\mu_e - \overline{\Delta}_1(\mu_A + \mu_e)]\lambda + \overline{\Delta}_2(E_2)\\ &\quad - \overline{\Delta}_1(E_2)\mu_A\mu_e = 0. \end{aligned} \tag{11}$$

Suppose that (11) has a pair of purely imaginary roots

$$\lambda_1 = i\omega_0 \quad \text{and} \quad \lambda_2 = -i\omega_0,$$

where $\omega_0 > 0$. Therefore, from the relationship between the root and coefficient of cubic equation, the third root of Eq. (11) is

$$\lambda_3 = \overline{\Delta}_1(E_2) - (\mu_A + \mu_e).$$

We choose α_e as the Hopf bifurcation parameter and take $\lambda_1 = i\omega_0$ into (11)

$$\begin{aligned} &-i\omega_0^3 - [\mu_A + \mu_e - \overline{\Delta}_1(E_2)]\omega_0^2\\ &\quad + i[\mu_A\mu_e - \overline{\Delta}_1(E_2)(\mu_A + \mu_e)]\omega_0\\ &\quad + \overline{\Delta}_2(E_2) - \overline{\Delta}_1(E_2)\mu_A\mu_e = 0. \end{aligned} \tag{12}$$

Separating the real and the imaginary parts of (12), we can get

$$\begin{cases} (\mu_A\mu_e - \overline{\Delta}_1(E_2)(\mu_A + \mu_e)t)\omega_0 - \omega_0^3 = 0,\\ \overline{\Delta}_2(E_2) - \overline{\Delta}_1(E_2)\mu_A\mu_e\\ \qquad - (\mu_A + \mu_e - \overline{\Delta}_1(E_2))\omega_0^2 = 0. \end{cases} \tag{13}$$

then

$$\begin{aligned} \omega_0 &= \sqrt{\mu_A\mu_e - \overline{\Delta}_1(E_2)(\mu_A + \mu_e)}\\ &= \sqrt{\frac{\overline{\Delta}_2(E_2) - \overline{\Delta}_2(E_2)\mu_A\mu_e}{(\mu_A + \mu_e - \overline{\Delta}_2(E_2))}}. \end{aligned}$$

Define

$$\begin{cases} B = \overline{\Delta}_2(E_2) - \overline{\Delta}_1(E_2)\mu_A\mu_e,\\ C = \mu_A + \mu_e - \overline{\Delta}_1(E_2),\\ D = \mu_A\mu_e - \overline{\Delta}_1(E_2)(\mu_A + \mu_e), \end{cases}$$

for convenience, we make the following assumption

(H1) $B > 0$, $C > 0$, $DC = B$.

When (H1) holds, we obtain the following critical value

$$\alpha_e^* = \frac{(M_2 + b)^2(M_2 + g) \times \left[\mu_A\mu_e(\mu_A + \mu_e) - \gamma_{\text{mel}}\left(1 - \frac{M_2}{k}\right)\frac{g}{M_2 + g}(\mu_A + \mu_e)^2 + \gamma_{\text{mel}}^2\left(1 - \frac{M_2}{k}\right)^2\frac{g}{M_2 + g}(\mu_A + \mu_e)\right]}{\alpha_A b M_2 \upsilon_{\text{mel}}}.$$

For mathematical convenience, we write the right end of the above equation as $\psi(g)$, that is $\alpha_e^* = \psi(g)$. Substitution of α_e^* in (12) yields

$$\mathrm{Re}(\lambda'(\alpha_e^*)) = \frac{\alpha_A \upsilon_{\mathrm{mel}} \dfrac{bM_2}{(M_2+b)^2(M_2+g)}[\mu_A\mu_e - \overline{\Delta}_1(E_2)(\mu_A+\mu_e) - 3\omega_0^2]}{[[\mu_A\mu_e - \overline{\Delta}_1(E_2)(\mu_A+\mu_e)] - 3\omega_0^2]^2 + 4[\mu_A\mu_e - \overline{\Delta}_1(E_2)]^2\omega_0^2}$$

and

(H2) $\mathrm{Re}(\lambda'(\alpha_e^*)) \neq 0$.

The existence of Hopf bifurcation is given by Theorem 6.

Theorem 6. *When (H1) and (H2) hold and $\alpha_e = \alpha_e^*$, the system (2) undergoes Hopf bifurcation at the equilibrium E_2.*

Substituting $A_1 = A - A_2$, $T_1 = T - T_2$, $M_1 = M - M_2$ into system (2) and rewriting A_1, T_1, M_1 as A, T, M, the system can be transformed into

$$\begin{pmatrix} \dfrac{\mathrm{d}A}{\mathrm{d}t} \\ \dfrac{\mathrm{d}T}{\mathrm{d}t} \\ \dfrac{\mathrm{d}M}{\mathrm{d}t} \end{pmatrix} = J \begin{pmatrix} A \\ T \\ M \end{pmatrix} + \begin{pmatrix} f_1 \\ f_2 \\ f_3 \end{pmatrix}, \tag{14}$$

where $f_1 = n_{11}M^2$, $f_2 = 0$, $f_3 = n_{12}TM + n_{13}M^2$ and

$$J_{E_2} = \begin{pmatrix} -\mu_A & 0 & \alpha_A \dfrac{b}{(M_2+b)^2} \\ \alpha_e^* & -\mu_e & 0 \\ 0 & -\upsilon_{\mathrm{mel}} \dfrac{M_2}{M_2+g} & \gamma_{\mathrm{mel}}\left(1 - \dfrac{2M_2}{k}\right) - \upsilon_{\mathrm{mel}} \dfrac{T_2M_2}{(M_2+g)^2} \end{pmatrix}.$$

The coefficients of f_1 and f_3 are

$$n_{11} = -\frac{2\alpha_A b}{(M_2+b)^2},$$

$$n_{12} = -\frac{2\upsilon_{\mathrm{mel}} g}{(M_2+b)^2},$$

$$n_{13} = -\frac{2\gamma_{\mathrm{mel}}}{k} + \upsilon_{\mathrm{mel}} \frac{2T_2 g}{(M_2+g)^3}.$$

The three-dimensional system (2) is further transformed into the two-dimensional form

$$\begin{pmatrix} \dfrac{\mathrm{d}x}{\mathrm{d}t} \\ \dfrac{\mathrm{d}y}{\mathrm{d}t} \end{pmatrix} = \begin{pmatrix} 0 & -\omega_0 \\ \omega_0 & 0 \end{pmatrix} \begin{pmatrix} x \\ y \end{pmatrix} + \begin{pmatrix} G_1 \\ G_2 \end{pmatrix}.$$

According to the ordinary differential Hopf bifurcation theory [Kuznetsov, 2013], we obtain

$$a(\alpha_e^*) = \frac{1}{16}[6rg_{13} + 2t(g_{13} + sg_{14}) + 2t(g_{23} + sg_{24}) + 6rg_{23}] + \frac{1}{16\omega_0(\alpha_e^*)}[2g_{12}(g_{11} + g_{15}) - 2g_{22}(g_{21} + g_{25}) - 4g_{11}g_{21} + 4g_{15}g_{25}].$$

See Appendix A.1 for coefficient value and detailed calculation process.

Theorem 7. *When $\alpha_e = \alpha_e^*$, the Hopf bifurcation of system (2) occurs at the positive equilibrium E_2, and if $a(\alpha_e^*) < 0$ ($a(\alpha_e^*) > 0$) is true, the bifurcation is supercritical (subcritical).*

3. Codimension Two Bifurcations

In the previous section, we have studied the existence of Hopf bifurcation and its corresponding bifurcation properties at the positive equilibrium point E_2 with α_e as the bifurcation parameter, but we are also interested in the influence of the interaction of α_e and g on the dynamic properties of system (2). In this section, we study the codimension two bifurcations, namely Bautin bifurcation and Bogdanov–Takens bifurcation, according to

[Zhang & Niu, 2020; Maleki *et al.*, 2010; Peng & Li, 2014], and finally give the existing conditions and the normal forms of the corresponding bifurcations.

3.1. *Bautin bifurcation*

According to the distribution of the roots of the cubic equation with one variable, when the parameter α_e is near α_e^*, there are $\xi(\alpha_e)$ and $\omega(\alpha_e)$, so that the characteristic equation has a pair of conjugate complex roots $\lambda(\alpha_e) = \xi(\alpha_e) \pm i\omega(\alpha_e)$, with $\xi(\alpha_e^*) = 0$, $\omega(\alpha_e^*) = \omega_0$. When the first Lyapunov coefficient $l_1(0) = 0$ and the second Lyapunov coefficient $l_2(0) \neq 0$, the Hopf bifurcation degenerates, and the Bautin bifurcation of system (2) occurs at the positive equilibrium E_2. Thus, we can get

$$l_1(0) = \frac{a(\alpha_e^*)}{\omega(\alpha_e^*)}.$$

We choose α_e and g as the bifurcation parameters and introduce a small perturbation $\mu = (\mu_1, \mu_2)$, that is, $\alpha_e = \alpha_e^* + \mu_1$, $g = g^* + \mu_2$, to the bifurcation parameters to calculate the second Lyapunov coefficient. According to [Zhang & Niu, 2020], we can calculate the expression of $l_2(0)$ (see Appendix A.2)

$$\begin{aligned}
12l_2(0) = {} & \frac{1}{\omega_0}\operatorname{Re} g_{32} + \frac{1}{\omega_0^2}\operatorname{Im}\left[g_{20}\overline{g}_{31} - g_{11}(4g_{31} + 3\overline{g}_{22}) - \frac{1}{3}g_{02}(g_{40} + \overline{g}_{13}) - g_{30}g_{12}\right] \\
& + \frac{1}{\omega_0^3}\operatorname{Re}\left[g_{20}\overline{g}_{11}(3g_{12} - \overline{g}_{30}) + g_{20}g_{02}\left(\overline{g}_{12} - \frac{1}{3}g_{30}\right) + \frac{1}{3}g_{20}\overline{g}_{02}g_{30} + g_{11}\overline{g}_{02}\left(\frac{5}{3}\overline{g}_{30} + 3g_{12}\right)\right] \\
& + \frac{1}{\omega_0^3}\operatorname{Re}\left[\frac{1}{3}g_{11}g_{02}\overline{g}_{03} - 4g_2^{11}g_{30}\right] + \frac{3}{\omega_0^3}\operatorname{Im}(g_{20}g_{11})\operatorname{Im} g_{21} + \frac{1}{\omega_0^4}\operatorname{Im}[g_{11}\overline{g}_{02}(\overline{g}_{20}^2 - 3\overline{g}_{20}g_{11} - 4g_{11}^2)] \\
& + \frac{1}{\omega_0^4}\operatorname{Im}(g_{20}g_{11})[3\operatorname{Re}(g_{20}g_{11}) - 2|g_{02}|^2].
\end{aligned}$$

The regularity of the map $\varphi : (\mu_1, \mu_2) \to (\frac{\xi(\mu)}{\omega(\mu)}, l_1(\mu))$ at $\mu = (0, 0)$ is actually

$$\text{(H3)} \quad \begin{vmatrix} \dfrac{\partial \dfrac{\xi(\mu)}{\omega(\mu)}}{\partial \mu_1} & \dfrac{\partial \dfrac{\xi(\mu)}{\omega(\mu)}}{\partial \mu_2} \\ \dfrac{\partial l_1(\mu)}{\partial \mu_1} & \dfrac{\partial l_1(\mu)}{\partial \mu_2} \end{vmatrix}_{\mu=0} \neq 0.$$

Theorem 8. *Assume that the conditions in Theorem 2(ii), and $l_1(0) = 0$ and hypothesis (H3) are all satisfied. The Hopf bifurcation will degenerate; That is, the system (2) undergoes Bautin bifurcation at the positive equilibrium E_2 with respect to the parameters α_e and g.*

Remark 3.1. Actually, according to [Kuznetsov, 2013], after nonlinear transformation, the system (2) is equivalent to the following Bautin bifurcation truncated normal form:

$$\dot{z} = (\beta_1 + i)z + \beta_2 z|z|^2 + sz|z|^4, \tag{15}$$

where $s = \operatorname{sign}(l_2(0)) = \pm 1$.

3.2. *Bogdanov–Takens bifurcation*

When the system satisfies both Hopf bifurcation and saddle-node bifurcation conditions at the instantaneous equilibrium point E_2^* or E_4^*, the Bogdanov–Takens bifurcation will appear. Without loss of generality, in this subsection, we study the Bogdanov–Takens bifurcation of the system at the positive equilibrium E_2^*. The characteristic equation of positive equilibrium point E_2^* is

$$\begin{aligned}
\lambda^3 + {} & [\mu_A + \mu_e - \overline{\Delta}_1(E_2^*)]\lambda^2 \\
& + [\mu_A\mu_e - \overline{\Delta}_1(E_2^*)(\mu_A + \mu_e)]\lambda + \overline{\Delta}_2(E_2^*) \\
& - \overline{\Delta}_1(E_2^*)\mu_A\mu_e = 0.
\end{aligned} \tag{16}$$

When the following conditions are true

$$\begin{cases} \overline{\Delta}_2(E_2^*) - \overline{\Delta}_1(E_2^*)\mu_A\mu_e = 0, \\ \mu_A\mu_e - \overline{\Delta}_1(E_2^*)(\mu_A + \mu_e) = 0, \end{cases} \tag{17}$$

then, the eigenvalues of (16) are $\lambda_1 = \lambda_2 = 0$ and $\lambda_3 = \overline{\Delta}_1(E_2^*) - (\mu_A + \mu_e)$. Thus, the Bogdanov–Takens bifurcation of system (2) appears at the positive equilibrium E_2^*. Let $\alpha_e = \alpha_e^{**}$ and $g = g^{**}$ be

the bifurcation parameter values, and the normal form of the original system at the equilibrium point E_2^* is computed (see Appendix A.3)

$$\begin{cases} \dfrac{\mathrm{d}u_1}{\mathrm{d}t} = u_2, \\ \dfrac{\mathrm{d}u_2}{\mathrm{d}t} = w_{11}u_1^2 + (2w_{11} + w_{22})u_1u_2 \\ \qquad\qquad + (w_{25} + w_{11})u_2^2 + O(|(u_1, u_2)|^3). \end{cases} \tag{18}$$

We calculate the universal folding of Bogdanov–Takens bifurcation by adding a disturbance to the bifurcation parameter, namely $g = g^{**} + \varepsilon_1$, $\alpha_e = \alpha_e^{**} + \varepsilon_2$. The transversality condition can be obtained by computing

$$\text{(H4)} \quad \left| \begin{matrix} \dfrac{\partial \phi_1}{\partial \varepsilon_1} & \dfrac{\partial \phi_1}{\partial \varepsilon_2} \\ \dfrac{\partial \phi_2}{\partial \varepsilon_1} & \dfrac{\partial \phi_2}{\partial \varepsilon_2} \end{matrix} \right|_{(\alpha_e, g) = (\alpha_e^{**} + \varepsilon_2, g^{**} + \varepsilon_1)} \neq 0.$$

Finally, the universal unfolding of Bogdanov–Takens bifurcation is written as

$$\begin{cases} \dfrac{\mathrm{d}u_1}{\mathrm{d}t} = u_2, \\ \dfrac{\mathrm{d}u_2}{\mathrm{d}t} = \phi_1(\varepsilon_1, \varepsilon_2)u_1 + \phi_2(\varepsilon_1, \varepsilon_2)u_2 + w_{11}u_1^2 \\ \qquad\qquad + (2w_{11} + w_{22})u_1u_2 + (w_{25} + w_{11})u_2^2. \end{cases} \tag{19}$$

Furthermore, we take $w_{25} = -w_{11}$ to eliminate the u_2^2 term

$$\begin{cases} \dot{u}_1 = u_2, \\ \dot{u}_2 = \tilde{\phi}_1(\varepsilon_1, \varepsilon_2)u_1 + \tilde{\phi}_2(\varepsilon_1, \varepsilon_2)u_2 \\ \qquad + \tilde{w}_{11}u_1^2 + su_1u_2, \end{cases} \tag{20}$$

where

$$s = \mathrm{sign}(2w_{11} + w_{22}) = \pm 1.$$

According to Bogdanov–Takens bifurcation normal form theory in [Kuznetsov, 2013], the homoclinic orbit expression of the original system can be calculated.

Theorem 9. *There is a unique smooth curve corresponding to the homoclinic bifurcation of the saddle point of system (15), which starts from the Bogdanov–Takens bifurcation point and has a local representation*

$$P = \left\{ (\tilde{\phi}_1, \tilde{\phi}_2) : \tilde{\phi}_1 = -\frac{6}{25}\tilde{\phi}_2 + o(\tilde{\phi}_2^2), \tilde{\phi}_2 < 0 \right\}.$$

4. Simulation

In this section, some parameters are selected for numerical simulation, so as to support the theoretical analysis results. System (2) is a three-dimensional system, which contains nine parameters. It is very difficult to study its properties in the whole nine-dimensional parameter space. From the previous analysis, we can see that the number of CD8+T cells and melanoma cells in patients with melanoma are very important for the development of melanoma, and the values of parameters α_e and g will directly affect the changes of the number of both. Therefore, the dynamic properties of system (2) in parameter (α_e–g)-plane are studied by fixing other parameters and selecting parameters α_e and g as bifurcation parameters.

We then choose different (α_e, g) to simulate the effect of homoclinic orbit and limit point of cycles on the periodic solution of the system as shown in Table 1. For example, it can be calculated that $B = 0.00439828 > 0$, $C = 0.530485 > 0$, $D = 0.00829114 > 0$, when $\alpha_e = 0.075604$ and $g = 1.05$, so the assumption (H1) can be satisfied. Furthermore, we can obtain $l_1(0) = 0.000903465 > 0$. The Hopf bifurcation of system (2) occurs at the positive equilibrium point E_2, and the bifurcation is supercritical. Figure 2 shows the corresponding bifurcation diagram of Table 1 in (α_e–T)-plane with different g, in which the saddle-node represents saddle-node bifurcation, and the system has stable or unstable periodic solutions near Hopf bifurcation. To prove the existence of homoclinic orbit, we fix $g = 1.285$ and change the value of α_e so that it passes through the left saddle-node bifurcation curve (SN_1), Hopf bifurcation curve, homoclinic bifurcation curve and right saddle-node bifurcation curve (SN_2) in turn (the relations of the parameters for differential bifurcations are shown in Table 2). We take the following value for α_e

$$D1 : 0.07659, \quad D2 : 0.07882, \quad D3 : 0.0794,$$

$$D4 : 0.081, \quad D5 : 0.092035.$$

When the value of α_e passes through the left saddle-node bifurcation curve (SN_1) and Hopf bifurcation curve, the periodic solution of the system will appear near the positive equilibrium point E_2, as

Table 1. The values of B, C and D in assumption (H1) with different (α_e, g).

(α_e, g)	B	C	D	$l_1(0)$
(a) (0.077439, 0.25)	0.01171628	0.55203955	0.02122373	−2.539441e−02
(b) (0.073981, 0.70)	0.00769940	0.54041220	0.01424732	−1.072887e−03
(c) (0.074053, 0.80)	0.00675559	0.53761002	0.01256601	−2.801619e−04
(d) (0.075604, 1.05)	0.00439828	0.53048520	0.00829114	9.034652e−04

shown in Fig. 3(b). Here, if the initial value of M is near E_2, and it will eventually converge to the stable periodic solution, otherwise, there is an unstable periodic solution, and the solution of the system will eventually be attracted to E_4. When α_e further increases and passes through the homoclinic bifurcation curve, the periodic solution of the system will disappear with the appearance of the homoclinic orbit, and when the initial value is near E_2, it will eventually be asymptotically stable to E_2 as shown

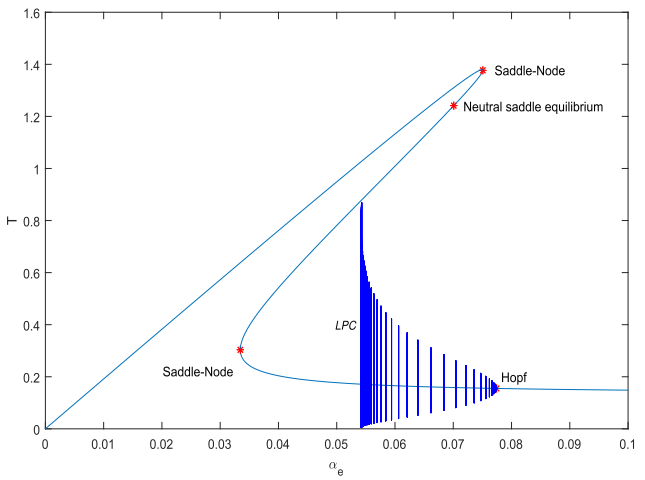

(a) $g = 0.25$

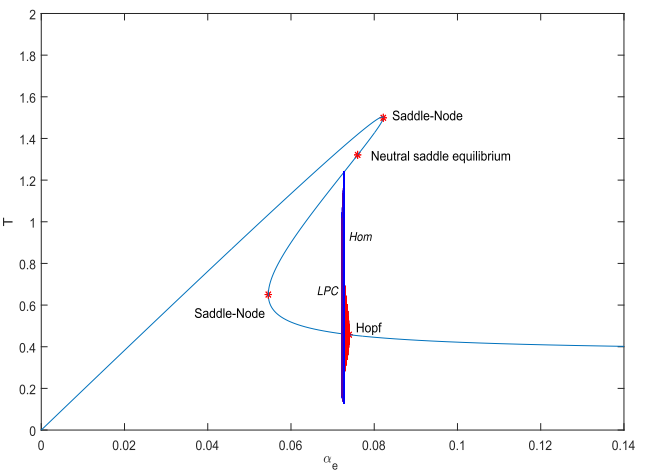

(b) $g = 0.7$

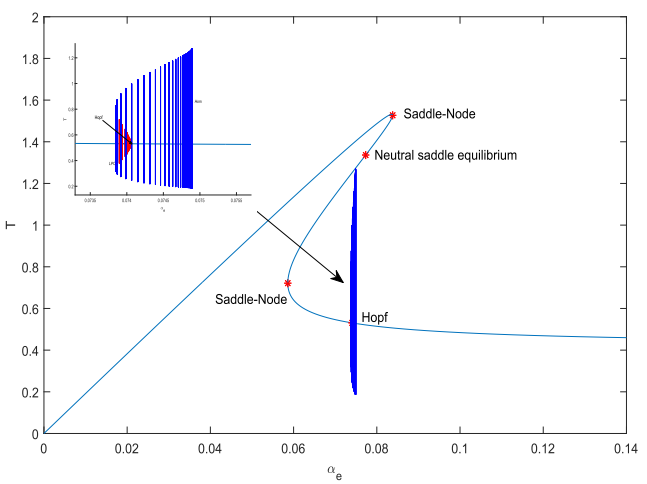

(c) $g = 0.8$

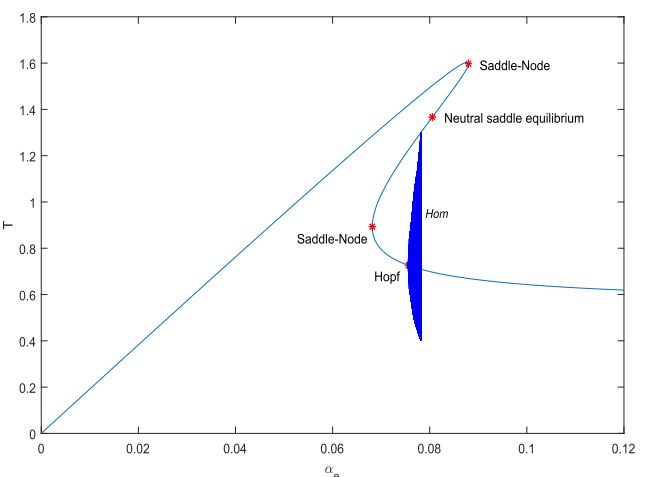

(d) $g = 1.05$

Fig. 2. Bifurcation diagram in $(\alpha_e$–$T)$-plane with different g. (a) One stable limit cycle bifurcates from supercritical Hopf bifurcation and disappears from Homoclinic bifurcation, (b) and (c) two limit cycles appear from the limit point of cycles, the unstable one disappearing from subcritical Hopf bifurcation and the stable one disappearing from homoclinic bifurcation and (d) one unstable limit cycle bifurcates from subcritical Hopf bifurcation and disappears from homoclinic bifurcation.

Table 2. The relations of the parameters α_e and g for bifurcation curve.

Bif Curves	The Implicit Expression of the Parameters α_e and g
SN_1	$b+g-k<0$, $P(M_c)=0$ and $\overline{\Delta}_2(E_2^*)=\overline{\Delta}_1(E_2^*)\mu_A\mu_e$
SN_2	$b+g-k<0$, $P(M_d)=0$ and $\overline{\Delta}_2(E_4^*)=\overline{\Delta}_1(E_4^*)\mu_A\mu_e$
H	(H1) $(B>0, C>0, DC=B)$, $\alpha_e^*=\psi(g)$ and (H2) $(R_e(\lambda'(\alpha_e^*))\neq 0)$
NE	$[\overline{\Delta}_1(E_2)(\mu_A+\mu_e)-\mu_A\mu_e][\mu_A+\mu_e-\overline{\Delta}_1(E_2)]=\overline{\Delta}_2(E_2)-\overline{\Delta}_1(E_2)\mu_A\mu_e$
LPC	$\beta_2^2+4\beta_1=0$, $\beta_2>0$
Hom	$\tilde{\phi}_1=-\frac{6}{25}\tilde{\phi}_2+o(\tilde{\phi}_2^2), \tilde{\phi}_2<0$

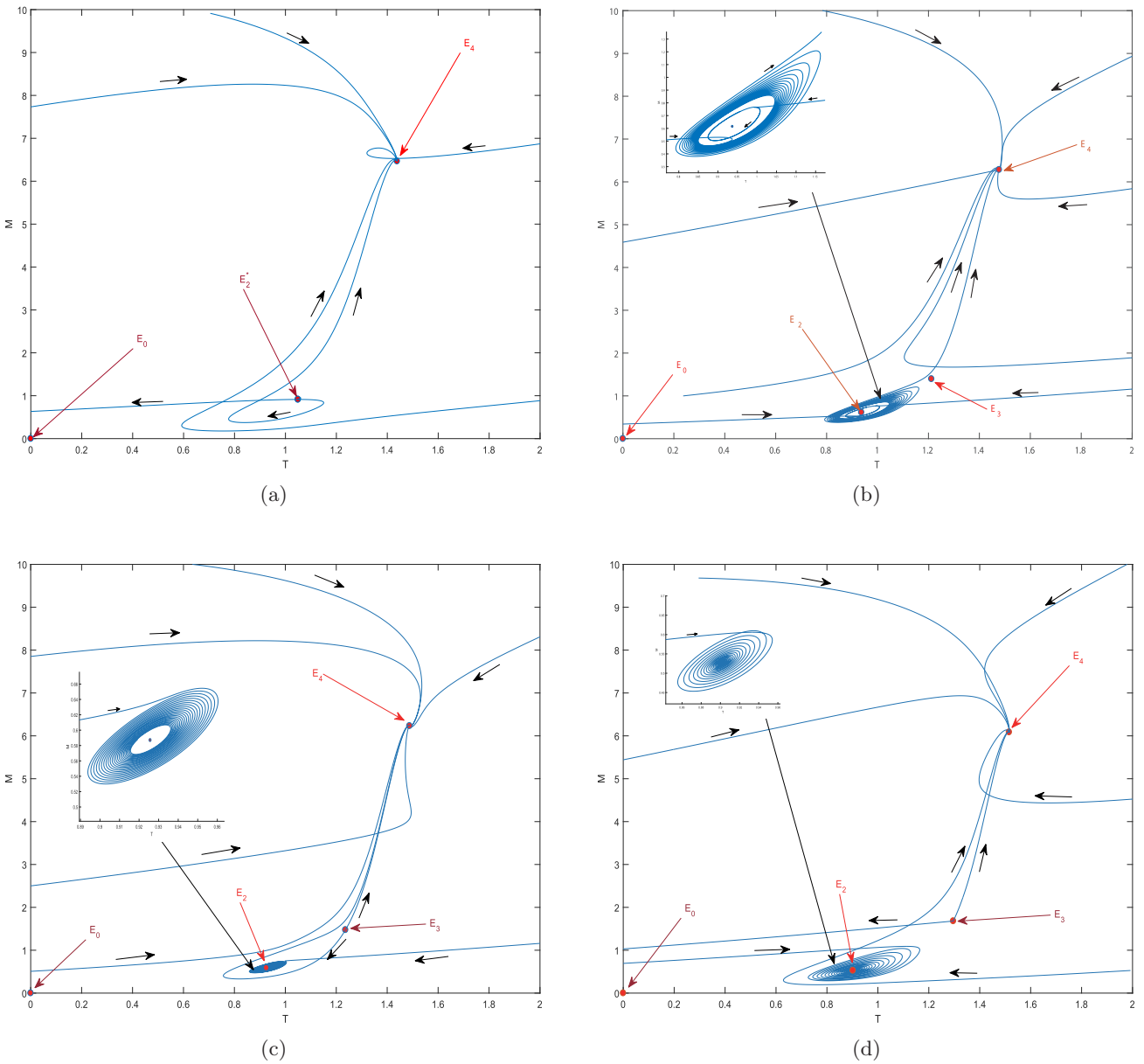

Fig. 3. Periodic solutions and trajectories of the system with different values of α_e in regions ($D1$–$D6$) of Fig. 1. (a) $D1:(\alpha_e,g)=(0.07659,1.285)$, (b) $D2:(\alpha_e,g)=(0.077,1.285)$, (c) $D3:(\alpha_e,g)=(0.07882,1.285)$, (d) $D4:(\alpha_e,g)=(0.0794,1.285)$, (e) $D5:(\alpha_e,g)=(0.081,1.285)$ and (f) $D6:(\alpha_e,g)=(0.0725,0.325)$.

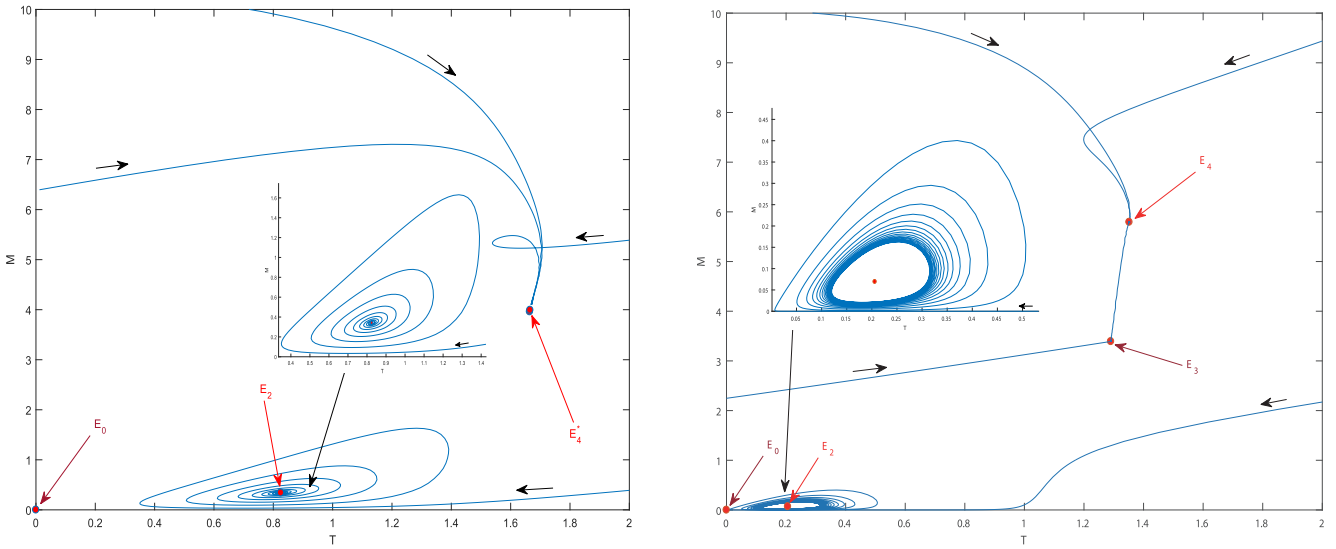

(e) (f)

Fig. 3. (*Continued*)

in Figs. 3(d) and 3(e). In Fig. 3(f), namely, region $D6$, there is a stable periodic solution near E_2.

When parameters $\alpha_e = 0.074192$ and $g = 0.845972$, there are first Lyapunov coefficient $l_1(0) = 0$ and second Lyapunov coefficient $l_2(0) \approx 0.00015$, and the transversality condition in hypothesis (H3) is $0.845997 \neq 0$. Thus, according to Theorem 8, system (2) undergoes Bautin bifurcation at the positive equilibrium point E_2. The supercritical Hopf bifurcation curve is above the point GH, and the subcritical Hopf bifurcation curve is below it, as shown in Fig. 1.

In Figs. 4 and 5, several phase portraits and their corresponding waveform graphs are obtained by selecting different values for the parameters in regions $D7$–$D10$ of Fig. 1. We choose different (α_e, g) values near GH point, and the numerical simulation results are shown in Fig. 4. In Fig. 4(a), when the parameters are set in the sharp region $D7$ surrounded by the limit points of cycles curve, homoclinic bifurcation curve and subcritical Hopf bifurcation curve, the system will appear with two unstable periodic solutions, one of which has larger amplitude but decreases with time, and the other

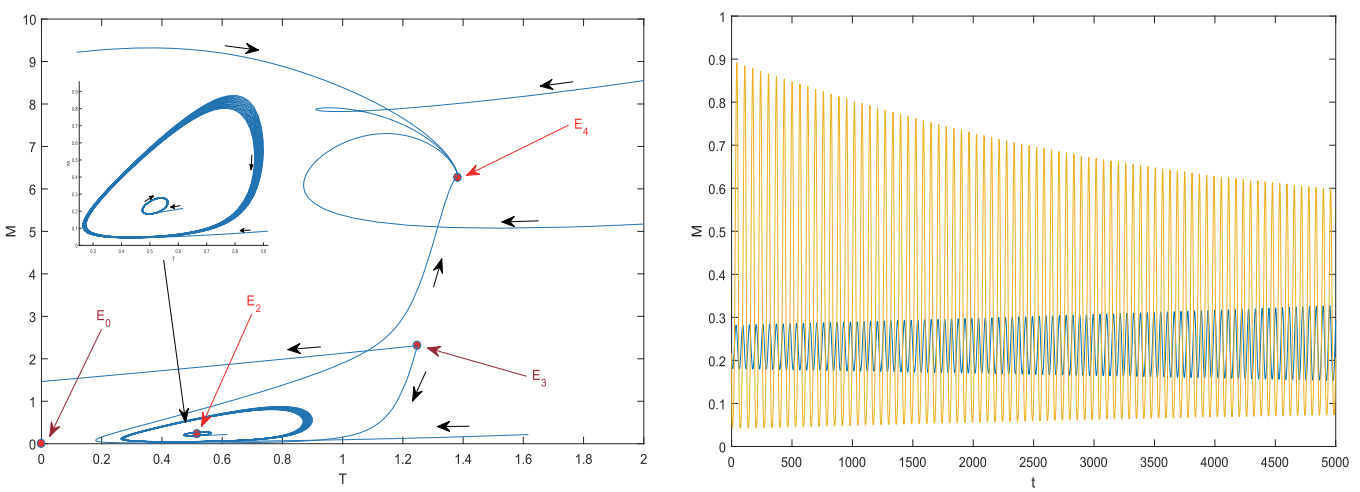

(a) $D7 : (\alpha_e, g) = (0.07375, 0.78)$

Fig. 4. Numerical results for system (2) in regions $D7$, $D8$ and GH point of Fig. 1. (a) Two unstable periodic solutions, one has larger amplitude but decreases with time, and the other has the opposite, (b) multiple stable periodic solutions and (c) one unstable periodic solution is ultimately attracted to E_4.

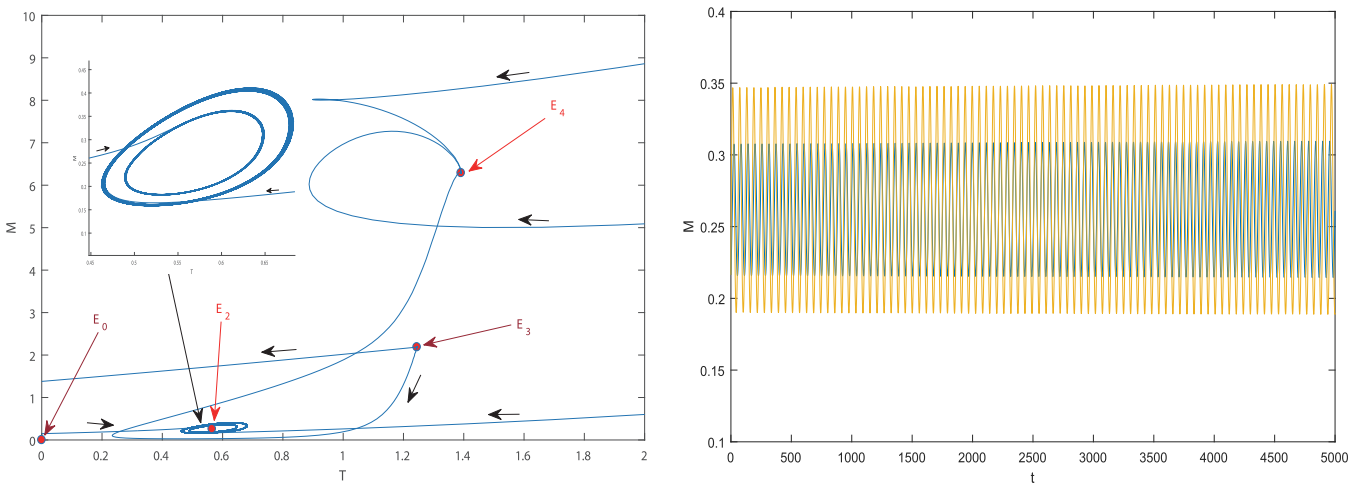

(b) GH : $(\alpha_e, g) = (0.07419, 0.8459)$

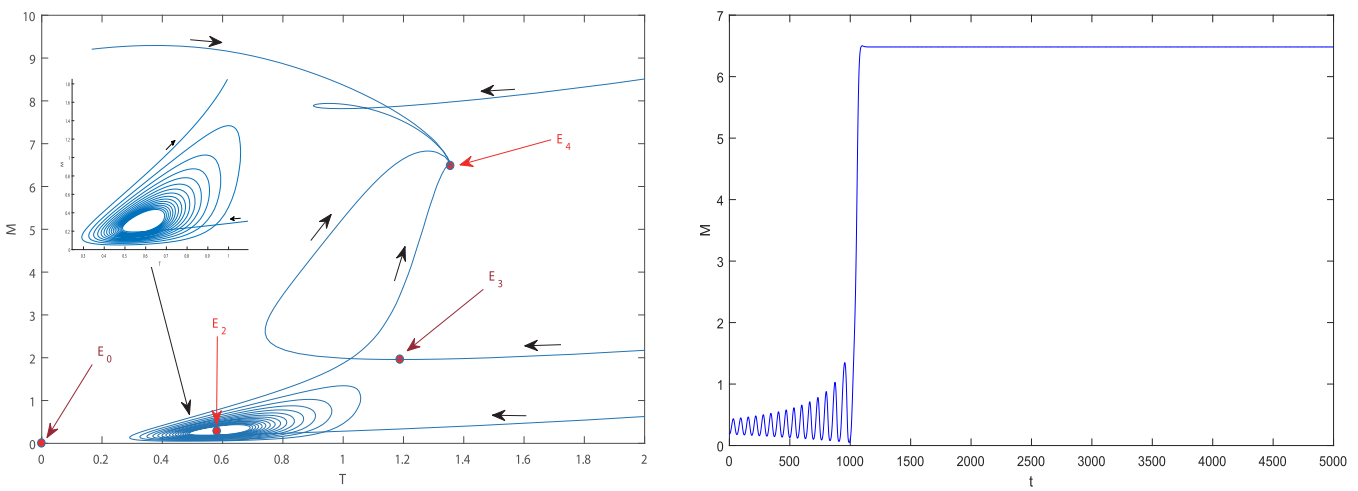

(c) $D8 : (\alpha_e, g) = (0.07219, 0.8559)$

Fig. 4. (*Continued*)

has the opposite. In Fig. 4(c), there is an unstable periodic solution in the system, and the solution will eventually be attracted to E_4. In this case, the number of tumor cells will eventually stabilize to constant values, namely E_4. Nevertheless, Fig. 4(b) indicates that system (2) has multiple stable periodic solutions at GH point. That is to say, when the initial number of tumor cells is small, the system will eventually oscillate at the equilibrium point E_2, while when the initial number of tumor cells is large, it will converge to the equilibrium point E_4. Moreover, there are also interesting periodic phenomena in regions $D9$ and $D10$, as shown in Fig. 5.

In general, the activation rate of CD8+T cells, the semi-saturation constant of tumor cells, and the number of initial melanoma and CD8+T cells will affect the final stable state of melanoma. From the simulation results, we know that the equilibrium point E_4 is always stable, but in this stable state, the number of melanoma cells is at a high level. This stability is not conducive to the improvement of the disease. Due to the emergence of various high codimension bifurcations, a stable periodic solution begins to appear near the positive equilibrium E_2 (see Figs. 3 and 4), which is conducive to the reduction of the number of melanoma cells, that is, the tumor will be in a benign state, which is the result we want to see.

Usually time delay effect can be considered in a tumor model, see [Wang *et al.*, 2013; Bi & Ruan,

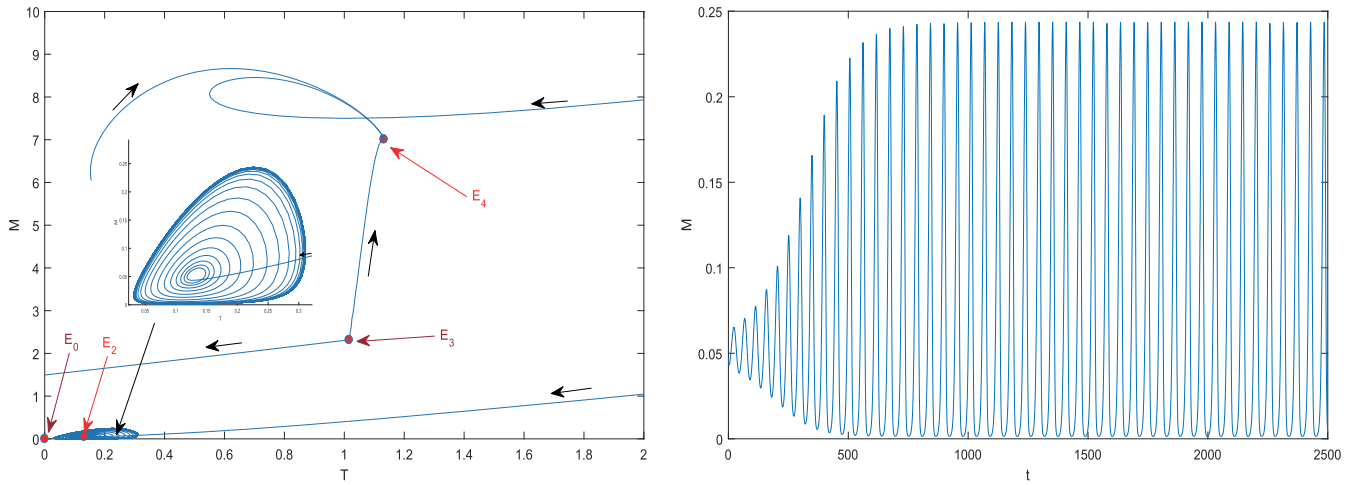

(a) $D9 : (\alpha_e, g) = (0.06, 0.2)$

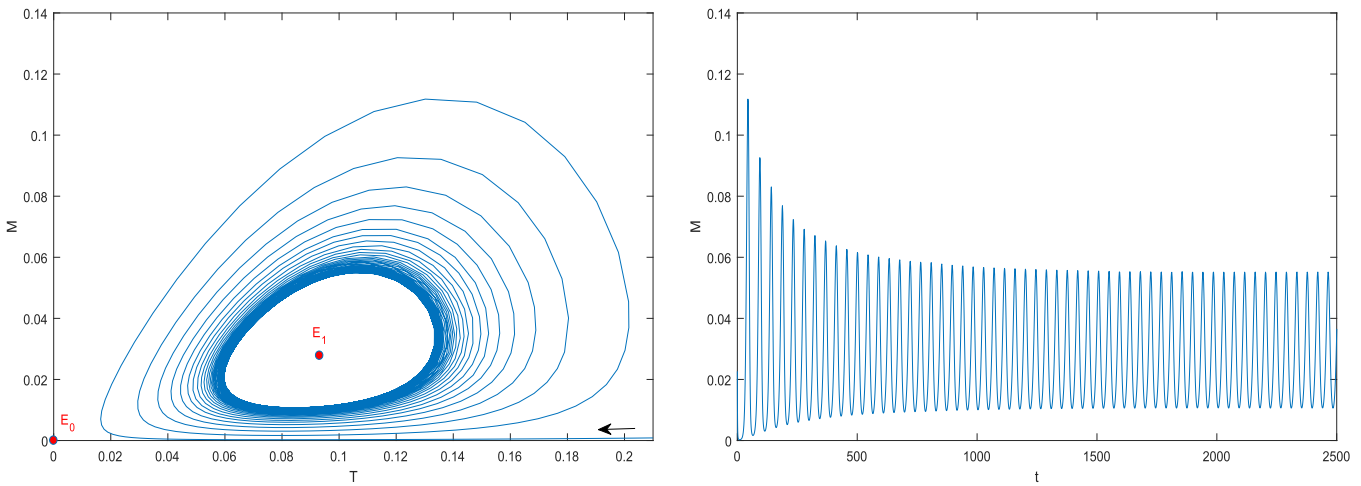

(b) $D10 : (\alpha_e, g) = (0.075, 0.15)$

Fig. 5. Numerical results for system (2) in regions $D9$ and $D10$ of Fig. 1. (a) One stable periodic solution stabilized by small amplitude and (b) one stable periodic solution stabilized by big amplitude.

2013]. For example, considering the delayed apoptosis of T cells in model (2), we have model (21). By using DDE-Biftool package [Engelborghs *et al.*, 2002; Verheyden, 2007], we conducted some simulations, and the bifurcation diagram in τ–g plane can be obtained as shown in Fig. 6. The results show that Bogdanov–Takens bifurcation and Bautin bifurcation also occur in the system, and the phenomenon of multistability and periodic coexistence still exists. The more interesting phenomenon is that Hopf–Hopf bifurcation and Zero-Hopf bifurcation appear in the positive parameter plane, which is not found in model (2). These bifurcation behaviors may induce more complicated dynamics in such a model, and is left as a future research

$$\begin{cases} \dfrac{dA}{dt} = \alpha_A \dfrac{M}{M+b} - \mu_A A, \\ \dfrac{dT}{dt} = \alpha_e A - \mu_e T(t-\tau), \\ \dfrac{dM}{dt} = \gamma_{\text{mel}} M \left(1 - \dfrac{M}{k}\right)(M-m) \\ \qquad\qquad - \upsilon_{\text{mel}} \dfrac{TM}{M+g}. \end{cases} \tag{21}$$

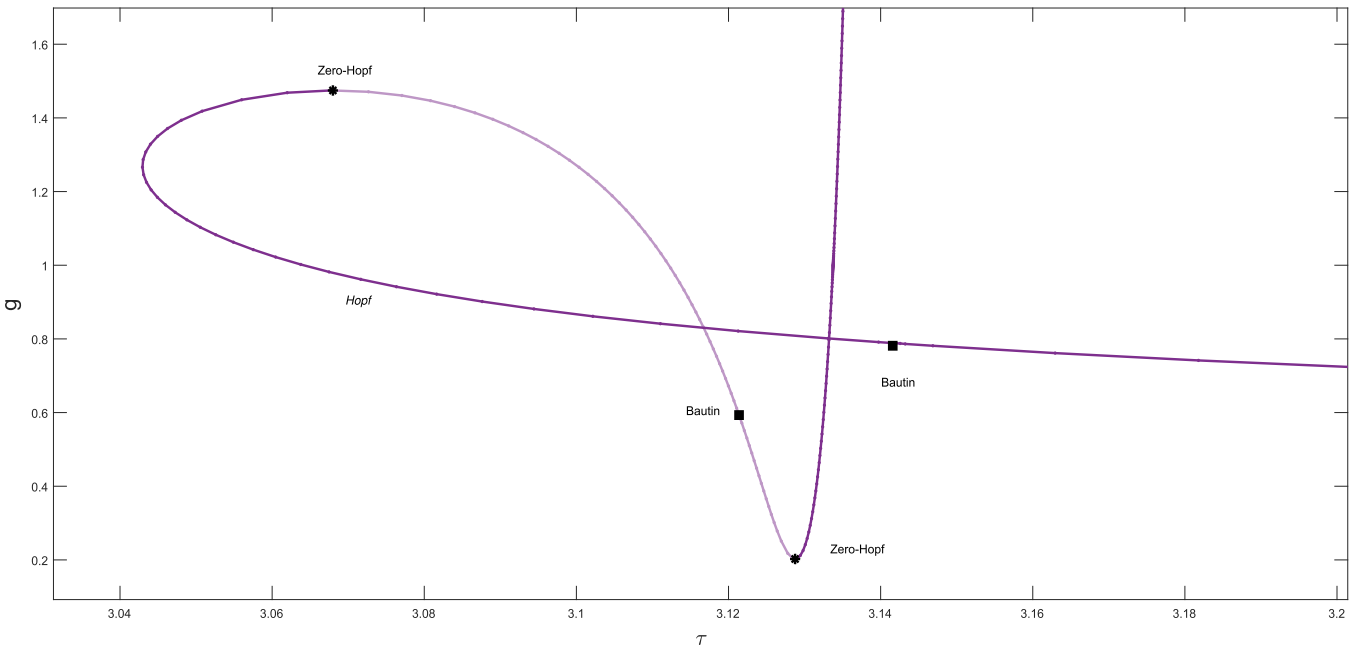

Fig. 6. Bifurcation diagram of delayed model (21) in (τ–g)-plane.

5. Conclusion and Discussion

In this paper, we studied the dynamic properties of a melanoma model with immune response. We analyzed the activation rate of CD8+T cells and the initial number of melanoma cells in patients with melanoma to study the final development of the disease. The dynamic properties of the model are mainly studied from the perspectives of equilibrium stability, Hopf bifurcation, Bogdanov–Takens bifurcation and Bautin bifurcation, and the theoretical results are finally explained by numerical simulation. Firstly, the non-negativity and boundedness of the solution are proved. On this basis, the existence, stability and codimension one bifurcations of positive equilibriums are studied. When there is only one positive equilibrium, the positive equilibrium is stable. When there are three positive equilibriums, there are two stable equilibria and one unstable equilibrium. It is proved that the system undergoes Hopf bifurcation at the positive equilibrium, and the properties of Hopf bifurcation under different parameters are given. It is proved that saddle-node bifurcation occurs when the positive equilibriums coincide. Secondly, the codimension two bifurcations of the system are studied. It is proved that the system exists with Bautin bifurcation and Bogdanov–Takens bifurcation. We calculate the expression of the second Lyapunov coefficient and the normal form of Bautin bifurcation. For Bogdanov–Takens bifurcation, we obtain the normal form and homoclinic orbit. Finally, different parameters are selected to simulate the theoretical results. The bifurcation diagram of the system is created with the parameters of the activation rate of CD8+T cells by antigen-presenting cells and the semi-saturation coefficient of melanoma cells. Then, the simulation results of Hopf bifurcating periodic solution is obtained by fixing parameters and constant changes, and with the appearance of Bogdanov–Takens bifurcation homoclinic orbit, the periodic solution will disappear. For the Bautin bifurcation, the existence and asymptotic stability of different periodic solutions are obtained by taking values near the Bautin bifurcation point. More specifically, several phase portraits and their corresponding waveform graphs are obtained by selecting different values for the parameters.

To sum up, simulating the immune reaction process of melanoma patients in different periods, we get that the system will appear with different dynamic phenomena by increasing the activation rate of CD8+T cells or reducing the apoptosis rate of CD8+T cells through appropriate immunotherapy. It was found that the final development of the disease was mainly related to the number of melanoma cells and the activation rate of CD8+T cells.

Considering the time delay effect of the human immune response, this model does not consider the effect of time delay. In the follow-up research process, this problem will be further studied.

Acknowledgment

The authors are grateful to all anonymous reviewers for their valuable comments, which provided great help for the improvement of the paper.

References

Agur, Z., Halevi-Tobias, K., Kogan, Y. & Shlagman, O. [2016] "Employing dynamical computational models for personalizing cancer immunotherapy," *Expert Opin. Biol. Ther.* **16**, 1373–1385.

Alvarez, R. F., Barbuto, J. A. & Venegeroles, R. [2019] "A nonlinear mathematical model of cell-mediated immune response for tumor phenotypic heterogeneity," *J. Theor. Biol.* **471**, 42–50.

Ashyani, A., RabieiMotlagh, O. & Mohammadinejad, H. [2018] "A mathematical approach to effects of CTLs on cancer virotherapy in the second injection of virus," *J. Theor. Biol.* **453**, 78–87.

Bi, P. & Ruan, S. [2013] "Bifurcations in delay differential equations and applications to tumor and immune system interaction models," *SIAM J. Appl. Dyn. Syst.* **12**, 1847–1888.

Bromley, S. K., Burack, W. R., Johnson, K. G., Somersalo, K., Sims, T. N., Sumen, C., Davis, M. M., Shaw, A. S., Allen, P. M. & Dustin, M. L. [2001] "The immunological synapse," *Ann. Rev. Immunol.* **19**, 375–396.

d'Onofrio, A. [2005] "A general framework for modeling tumor-immune system competition and immunotherapy: Mathematical analysis and biomedical inferences," *Physica D* **208**, 220–235.

Engelborghs, K., Luzyanina, T. & Roose, D. [2002] "Numerical bifurcation analysis of delay differential equations using DDE-BIFTOOL," *ACM T. Math. Softw.* **28**, 1–21.

Friedman, R. J., Rigel, D. S. & Kopf, A. W. [1985] "Early detection of malignant melanoma: The role of physician examination and self-examination of the skin," *CA-Cancer J. Clin.* **35**, 130–151.

Hargadon, K. M., Johnson, C. E. & Williams, C. J. [2018] "Immune checkpoint blockade therapy for cancer: An overview of FDA-approved immune checkpoint inhibitors," *Int. Immunopharmacol.* **62**, 29–39.

Hu, X., Yuan, L. & Ma, T. [2020] "Mechanisms of JAK-STAT signaling pathway mediated by CXCL8 gene silencing on epithelial-mesenchymal transition of human cutaneous melanoma cells," *Oncol. Lett.* **20**, 1973–1981.

Karimkhani, C., Green, A. C., Nijsten, T., Weinstock, M., Dellavalle, R. P., Naghavi, M. & Fitzmaurice, C. [2017] "The global burden of melanoma: Results from the global burden of disease study 2015," *Br. J. Dermatol.* **177**, 134–140.

Kuznetsov, Y. A. [2013] *Elements of Applied Bifurcation Theory*, Vol. 112 (Springer Science & Business Media).

Li, J., Men, K., Yang, Y. & Li, D. [2015] "Dynamical analysis on a chronic hepatitis c virus infection model with immune response," *J. Theor. Biol.* **365**, 337–346.

Lim, S., Phillips, J. B., Da Silva, L. M., Zhou, M., Fodstad, O., Owen, L. B. & Tan, M. [2017] "Interplay between immune checkpoint proteins and cellular metabolism," *Cancer Res.* **77**, 1245–1249.

Makhlouf, A. M., El-Shennawy, L. & Elkaranshawy, H. A. [2020] "Mathematical modeling for the role of CD4+T cells in tumor-immune interactions," *Comput. Math. Method. M* **2020**.

Maleki, F., Beheshti, B., Hajihosseini, A. & Lamooki, G. R. R. [2010] "The Bogdanov–Takens bifurcation analysis on a three dimensional recurrent neural network," *Neurocomputing* **73**, 3066–3078.

Peng, G. & Li, C. [2014] "Computation of universal unfolding of the double zero bifurcation in the Z 2-symmetric system," *Int. J. Comput. Math.* **91**, 461–479.

Shan, C. & Zhu, H. [2014] "Bifurcations and complex dynamics of an SIR model with the impact of the number of hospital beds," *J. Diff. Eqs.* **257**, 1662–1688.

Terushkin, V. & Halpern, A. C. [2009] "Melanoma early detection," *Hematol. Oncol. Clin.* **23**, 481–500.

Tsur, N., Kogan, Y., Rehm, M. & Agur, Z. [2020] "Response of patients with melanoma to immune checkpoint blockade–insights gleaned from analysis of a new mathematical mechanistic model," *J. Theor. Biol.* **485**, 110033.

Verheyden, K. [2007] "New functionality in DDE-BIFTOOL v. 2.03. addendum to the manual of DDE-BIFTOOL v. 2.00 (and v. 2.02)."

Villani, A., Fabbrocini, G., Costa, C. & Scalvenzi, M. [2020] "Melanoma screening days during the coronavirus disease 2019 (covid-19) pandemic: Strategies to adopt," *Dermatol. Ther.* **10**, 525–527.

Wang, Y., Tian, J. P. & Wei, J. [2013] "Lytic cycle: A defining process in oncolytic virotherapy," *Appl. Math. Model.* **37**, 5962–5978.

Wang, J., Zheng, H. & Jia, Y. [2020] "Existence and bifurcation of non-constant positive steady states for a tumor-immune model," *Z. Angew. Math. Phys.* **71**, 1–24.

Yu, M., Dong, Y. & Takeuchi, Y. [2017] "Dual role of delay effects in a tumour-immune system," *J. Biol. Dyn.* **11**, 334–347.

Yu, J. & Jang, S. R. [2019] "A mathematical model of tumor-immune interactions with an immune checkpoint inhibitor," *Appl. Math. Comput.* **362**, 124523.
Zeng, C. & Ma, S. [2020] "Dynamic analysis of a tumor-immune system under ALLEE effect," *Math. Probl. Eng.* **2020**.
Zhang, H. & Niu, B. [2020] "Dynamics in a plankton model with toxic substances and phytoplankton harvesting," *Int. J. Bifurcation and Chaos* **30**, 2050035-1–21.

Appendix A

A.1. *Calculation of $a(\alpha_e^*)$*

Substituting

$$A_1 = A - A_2, \quad T_1 = T - T_2, \quad M_1 = M - M_2$$

into system (2) and rewriting A_1, T_1, M_1 as A, T, M, the system can be transformed into

$$\begin{pmatrix} \dfrac{\mathrm{d}A}{\mathrm{d}t} \\ \dfrac{\mathrm{d}T}{\mathrm{d}t} \\ \dfrac{\mathrm{d}M}{\mathrm{d}t} \end{pmatrix} = J_{E_2} \begin{pmatrix} A \\ T \\ M \end{pmatrix} + \begin{pmatrix} f_1 \\ f_2 \\ f_3 \end{pmatrix}, \tag{A.1}$$

where

$$f_1 = n_{11}M^2, \quad f_2 = 0, \quad f_3 = n_{12}TM + n_{13}M^2$$

and

$$J_{E_2} = \begin{pmatrix} -\mu_A & 0 & \alpha_A \dfrac{b}{(M_2+b)^2} \\ \alpha_e^* & -\mu_e & 0 \\ 0 & -\upsilon_{\mathrm{mel}} \dfrac{M_2}{M_2+g} & \gamma_{\mathrm{mel}}\left(1 - \dfrac{2M_2}{k}\right) - \upsilon_{\mathrm{mel}} \dfrac{T_2 M_2}{(M_2+g)^2} \end{pmatrix}.$$

The coefficients of f_1 and f_3 are

$$n_{11} = -\frac{2\alpha_A b}{(M_2+b)^2}, \quad n_{12} = -\frac{2\upsilon_{\mathrm{mel}} g}{(M_2+b)^2},$$

$$n_{13} = -\frac{2\gamma_{\mathrm{mel}}}{k} + \upsilon_{\mathrm{mel}} \frac{2T_2 g}{(M_2+g)^3}.$$

Let v_1, v_3 be the eigenvectors of the eigenvalues $\lambda_1 = i\omega_0$, $\lambda_3 = \overline{\Delta}_1(E_2) - (\mu_A + \mu_e)$, respectively, and we have

$$v_1 = \begin{pmatrix} 1 \\ \dfrac{\alpha_e\mu_e + i\alpha_e\omega_0}{\omega_0^2 + \mu_e^2} \\ \dfrac{\mu_A(M_2+b)^2 + i\omega_0(M_2+b)^2}{\alpha_A b} \end{pmatrix},$$

$$v_3 = \begin{pmatrix} \dfrac{\overline{\Delta}_1(E_2) - \mu_A}{\alpha_e} \\ 1 \\ \dfrac{(\overline{\Delta}_1(E_2) - \mu_e)(\overline{\Delta}_1(E_2) - \mu_A)(M_2+b)^2}{\alpha_e\alpha_A b} \end{pmatrix}.$$

Thus, the matrix $P = (\mathrm{Re}(v_1), \mathrm{Im}(v_1), v_3)$ is determined as follows

$$P = \begin{pmatrix} 1 & 0 & c \\ a & j & 1 \\ d & e & f \end{pmatrix},$$

where

$$a = \frac{\alpha_e\mu_e}{\omega_0^2 + \mu_e^2}, \quad j = \frac{\alpha_e\omega_0}{\omega_0^2 + \mu_e^2},$$

$$c = \frac{\overline{\Delta}_1(E_2) - \mu_A}{\alpha_e},$$

$$d = \frac{\mu_A(M_2+b)^2}{\alpha_A b}, \quad e = \frac{\omega_0(M_2+b)^2}{\alpha_A b},$$

$$f = \frac{(\overline{\Delta}_1(E_2) - \mu_e)(\overline{\Delta}_1(E_2) - \mu_A)(M_2+b)^2}{\alpha_e\alpha_A b}.$$

The inverse matrix of P is obtained

$$P^{-1} = \begin{pmatrix} p_{11} & p_{12} & p_{13} \\ p_{21} & p_{22} & p_{23} \\ p_{31} & p_{32} & p_{33} \end{pmatrix},$$

where

$$p_{11} = \frac{e - jf}{e - jf - ace + cdj},$$

$$p_{12} = \frac{-ce}{e - jf - ace + cdj},$$

$$p_{13} = \frac{cj}{e - jf - ace + cdj},$$

$$p_{21} = \frac{-d + af}{e - jf - ace + cdj},$$

$$p_{22} = \frac{-f + cd}{e - jf - ace + cdj},$$

$$p_{23} = \frac{-ac + 1}{e - jf - ace + cdj},$$

$$p_{31} = \frac{-ae + dj}{e - jf - ace + cdj},$$

$$p_{32} = \frac{e}{e - jf - ace + cdj},$$

$$p_{33} = \frac{-j}{e - jf - ace + cdj}.$$

By the linear transformation

$$\begin{pmatrix} x \\ y \\ z \end{pmatrix} = P \begin{pmatrix} A \\ T \\ M \end{pmatrix},$$

system (2) is converted to

$$\begin{pmatrix} \dfrac{\mathrm{d}x}{\mathrm{d}t} \\ \dfrac{\mathrm{d}y}{\mathrm{d}t} \\ \dfrac{\mathrm{d}z}{\mathrm{d}t} \end{pmatrix} = \begin{pmatrix} 0 & -\omega_0 & 0 \\ \omega_0 & 0 & 0 \\ 0 & 0 & \overline{\Delta}_1(E_2) - (\mu_A + \mu_e) \end{pmatrix} \begin{pmatrix} x \\ y \\ z \end{pmatrix} + \begin{pmatrix} g_1 \\ g_2 \\ g_3 \end{pmatrix},$$

where

$$g_1 = g_{11}x^2 + g_{12}xy + g_{13}xz + g_{14}yz + g_{15}y^2 + g_{16}z^2,$$

$$g_2 = g_{21}x^2 + g_{22}xy + g_{23}xz + g_{24}yz + g_{25}y^2 + g_{26}z^2,$$

$$g_3 = g_{31}x^2 + g_{32}xy + g_{33}xz + g_{34}yz + g_{35}y^2 + g_{36}z^2$$

and the coefficients of g_1, g_2, and g_3 are

$$g_{11} = (n_{11} + cn_{13})p_{31}^2 + cn_{12}p_{21}p_{31},$$

$$g_{12} = 2(n_{11} + cn_{13})p_{31}p_{32} + cn_{12}(p_{21}p_{32} + p_{22}p_{31}),$$

$$g_{13} = 2(n_{11} + cn_{13})p_{31}p_{33} + cn_{12}(p_{21}p_{33} + p_{23}p_{31}),$$

$$g_{14} = 2(n_{11} + cn_{13})p_{33}p_{32} + cn_{12}(p_{22}p_{33} + p_{23}p_{32}),$$

$$g_{15} = (n_{11} + cn_{13})p_{32}^2 + cn_{12}p_{22}p_{32},$$

$$g_{16} = (n_{11} + cn_{13})p_{33}^2 + cn_{12}p_{23}p_{33},$$

$$g_{21} = (an_{11} + n_{13})p_{31}^2 + n_{12}p_{21}p_{31},$$

$$g_{22} = 2(an_{11} + n_{13})p_{31}p_{32} + n_{12}(p_{21}p_{32} + p_{22}p_{31}),$$

$$g_{23} = 2(an_{11} + n_{13})p_{31}p_{33} + n_{12}(p_{21}p_{33} + p_{23}p_{31}),$$

$$g_{24} = 2(an_{11} + n_{13})p_{33}p_{32} + n_{12}(p_{22}p_{33} + p_{23}p_{32}),$$

$$g_{25} = (an_{11} + n_{13})p_{32}^2 + n_{12}p_{22}p_{32},$$

$$g_{26} = (an_{11} + n_{13})p_{33}^2 + n_{12}p_{23}p_{33},$$

$$g_{31} = (dn_{11} + fn_{13})p_{31}^2 + fn_{12}p_{21}p_{31},$$

$$g_{32} = 2(dn_{11} + fn_{13})p_{31}p_{32} + fn_{12}(p_{21}p_{32} + p_{22}p_{31}),$$

$$g_{33} = 2(dn_{11} + fn_{13})p_{31}p_{33} + fn_{12}(p_{21}p_{33} + p_{23}p_{31}),$$

$$g_{34} = 2(dn_{11} + fn_{13})p_{33}p_{32} + fn_{12}(p_{22}p_{33} + p_{23}p_{32}),$$

$$g_{35} = (dn_{11} + fn_{13})p_{32}^2 + fn_{12}p_{22}p_{32},$$

$$g_{36} = (dn_{11} + fn_{13})p_{33}^2 + fn_{12}p_{23}p_{33}.$$

Now, considering the center manifold

$$W_{\mathrm{loc}}^c(0) = \{(x, y, z) \in \mathbb{R}_+^3 \mid z = h(x, y), \\ |x| < \delta_1, |y| < \delta_2, h(0, 0) = 0\},$$

for δ_1, δ_2 sufficiently small, we assume that $h(x, y)$ has the following form

$$z = h(x, y) = rx^2 + sxy + ty^2 + \text{h.o.t.}$$

Then, we have

$$\frac{dz}{dt} = 2rx\frac{dx}{dt} + sx\frac{dy}{dt} + sy\frac{dx}{dt} + 2ty\frac{dy}{dt} \\ = [\overline{\Delta}_1(E_2) - (\mu_A + \mu_e)]z + g_3,$$

namely,

$$[\overline{\Delta}_1(E_2) - (\mu_A + \mu_e)](rx^2 + sxy + ty^2) + g_{31}x^2 \\ + g_{32}xy + g_{33}xz + g_{34}yz + g_{35}y^2 + g_{36}z^2 \\ = 2rx(-\omega_0 + g_1) + sx(\omega_0 x + g_2) \\ + sy(-\omega_0 y + g_1) + 2ty(\omega_0 x + g_2).$$

By comparing the coefficients of x^2, xy and y^2 on the left and right sides of the above formula, we can get

$$[\overline{\Delta}_1(E_2)-(\mu_A+\mu_e)]r+g_{31}=s\omega_0,\quad [\overline{\Delta}_1(E_2)-(\mu_A+\mu_e)]s+g_{32}=2(t-r)\omega_0,$$
$$[\overline{\Delta}_1(E_2)-(\mu_A+\mu_e)]t+g_{35}=-s\omega_0.$$

The following coefficients are obtained

$$r=\left[-\frac{g_{31}+g_{35}}{\overline{\Delta}_1(E_2)-(\mu_A+\mu_e)}-\frac{g_{32}\omega_0[\overline{\Delta}_1(E_2)-(\mu_A+\mu_e)]-g_{35}[\overline{\Delta}_1(E_2)-(\mu_A+\mu_e)]^2-2\omega_0^2(g_{31}+g_{35})}{[\overline{\Delta}_1(E_2)-(\mu_A+\mu_e)][4\omega_0^2+(\overline{\Delta}_1(E_2)-(\mu_A+\mu_e))^3]}\right],$$

$$s=-\frac{1}{\omega_0}\left[\frac{g_{32}\omega_0[\overline{\Delta}_1(E_2)-(\mu_A+\mu_e)]-g_{35}[\overline{\Delta}_1(E_2)-(\mu_A+\mu_e)]^2-2\omega_0^2(g_{31}+g_{35})}{4\omega_0^2+[\overline{\Delta}_1(E_2)-(\mu_A+\mu_e)]^3}+g_{35}\right],$$

$$t=\frac{g_{32}\omega_0[\overline{\Delta}_1(E_2)-(\mu_A+\mu_e)]-g_{35}[\overline{\Delta}(E_2)_1-(\mu_A+\mu_e)]^2-2\omega_0^2(g_{31}+g_{35})}{[\overline{\Delta}_1(E_2)-(\mu_A+\mu_e)][4\omega_0^2+(\overline{\Delta}_1(E_2)-(\mu_A+\mu_e))^3]}.$$

The three-dimensional system (2) is further transformed into the two-dimensional form

$$\begin{pmatrix}\dfrac{\mathrm{d}x}{\mathrm{d}t}\\[2ex]\dfrac{\mathrm{d}y}{\mathrm{d}t}\end{pmatrix}=\begin{pmatrix}0&-\omega_0\\ \omega_0&0\end{pmatrix}\begin{pmatrix}x\\y\end{pmatrix}+\begin{pmatrix}G_1\\G_2\end{pmatrix},$$

where

$$G_1=g_{11}x^2+g_{12}xy+g_{15}y^2+(sg_{13}+rg_{14})x^2y+(tg_{13}+sg_{14})xy^2+rg_{13}x^3+tg_{14}y^3,$$
$$G_2=g_{21}x^2+g_{22}xy+g_{25}y^2+(sg_{23}+rg_{24})x^2y+(tg_{23}+sg_{24})xy^2+rg_{23}x^3+tg_{24}y^3.$$

Thus,

$$G^1_{xx}=2g_{11}+2(sg_{13}+rg_{14})y+6rg_{13}x,$$
$$G^2_{xx}=2g_{21}+2(sg_{23}+rg_{24})y+6rg_{23}x,$$
$$G^1_{xy}=g_{12}+2(sg_{13}+rg_{14})x+2t(g_{13}+sg_{14})y,$$
$$G^2_{xy}=g_{22}+2(sg_{23}+rg_{24})x+2t(g_{23}+sg_{24})y,$$
$$G^1_{yy}=2g_{15}+2(tg_{13}+sg_{14})x+6tg_{14}y,$$
$$G^2_{yy}=2g_{25}+2(tg_{23}+sg_{24})x+6tg_{24}y,$$
$$G^1_{xxy}=2(sg_{23}+rg_{24}),$$
$$G^1_{xyy}=2(tg_{13}+sg_{14}),$$
$$G^2_{yyy}=6tg_{24},$$
$$G^2_{xxy}=2(sg_{23}+rg_{24}).$$

According to the ordinary differential Hopf bifurcation theory [Kuznetsov, 2013], we obtain

$$\begin{aligned}a(\alpha_e^*)=&\frac{1}{16}[6rg_{13}+2t(g_{13}+sg_{14})\\&+2t(g_{23}+sg_{24})+6rg_{23}]\\&+\frac{1}{16\omega_0(\alpha_e^*)}[2g_{12}(g_{11}+g_{15})\\&-2g_{22}(g_{21}+g_{25})-4g_{11}g_{21}+4g_{15}g_{25}].\end{aligned}$$

A.2. *Calculation of $l_2(0)$*

We choose α_e and g as the bifurcation parameters and introduce a small perturbation $\mu=(\mu_1,\mu_2)$, that is $\alpha_e=\alpha_e^*+\mu_1$, $g=g^*+\mu_2$, to the bifurcation parameters to calculate the second Lyapunov coefficient. We translate equilibrium E_2 to the origin by letting $A_3=A-A_2$, $T_3=T-T_2$, $M_3=M-M_2$

$$\begin{cases}\dfrac{\mathrm{d}A}{\mathrm{d}t}=\alpha_A\dfrac{M+M_2}{M+M_2+b}-\mu_A(A+A_2),\\[2ex]\dfrac{\mathrm{d}T}{\mathrm{d}t}=(\alpha_e^*+\mu_1)(A+A_2)-\mu_e(T+T_2),\\[2ex]\dfrac{\mathrm{d}M}{\mathrm{d}t}=\gamma_{\mathrm{mel}}(M+M_2)\left(1-\dfrac{M+M_2}{k}\right)\\[2ex]\qquad\qquad-\upsilon_{\mathrm{mel}}\dfrac{(T+T_2)(M+M_2)}{M+M_2+g^*+\mu_2}.\end{cases}\tag{A.2}$$

Denote $u=(A,T,M)^T$ and rewrite system (A.2) as

$$\dot{u}=f(u,\mu)=J_{E_2}(\mu)u+F(u,\mu),\tag{A.3}$$

where

$$J_{E_2} = \begin{pmatrix} -\mu_A & 0 & \alpha_A \dfrac{b}{(M_2+b)^2} \\ \alpha_e^* + \mu_1 & -\mu_e & 0 \\ 0 & -\upsilon_{\text{mel}} \dfrac{M_2}{M_2+g^*+\mu_2} & \gamma_{\text{mel}}\left(1-\dfrac{2M_2}{k}\right) - \upsilon_{\text{mel}} \dfrac{T_2(g^*+\mu_2)}{(M_2+g^*+\mu_2)^2} \end{pmatrix}$$

and

$$\begin{aligned} F(u,\mu) &= (F^1(u,\mu), F^2(u,\mu), F^3(u,\mu))^T \\ &= \frac{1}{2}B(u,u,\mu) + \frac{1}{6}C(u,u,u,\mu) + \frac{1}{24}D(u,u,u,u,\mu) + \frac{1}{120}E(u,u,u,u,u,\mu) + \text{h.o.t.} \end{aligned}$$

here, $u_i = (u_i^{(1)}, u_i^{(2)}, u_i^{(3)})^T$, $i = 1,2,3,4,5$,

$$B(u_1,u_2,\mu) = \begin{pmatrix} 0 \\ 0 \\ e_{20} \end{pmatrix} (u_1^{(3)}u_2^{(2)} + u_1^{(2)}u_2^{(3)}) + \begin{pmatrix} c_{21} \\ 0 \\ e_{21} \end{pmatrix} u_1^{(3)}u_2^{(3)},$$

$$C(u_1,u_2,u_3,\mu) = \begin{pmatrix} 0 \\ 0 \\ e_{30} \end{pmatrix} (u_1^{(2)}u_2^{(3)}u_3^{(3)} + u_1^{(3)}u_2^{(2)}u_3^{(3)} + u_1^{(3)}u_2^{(3)}u_3^{(2)}) + \begin{pmatrix} c_{31} \\ 0 \\ e_{21} \end{pmatrix} u_1^{(3)}u_2^{(3)}u_3^3,$$

$$\begin{aligned} D(u_1,u_2,u_3,u_4,\mu) = &\begin{pmatrix} 0 \\ 0 \\ e_{40} \end{pmatrix} (u_1^{(2)}u_2^{(3)}u_3^{(3)}u_4^{(3)} + u_1^{(3)}u_2^{(2)}u_3^{(3)}u_4^{(3)} + u_1^{(3)}u_2^{(3)}u_3^{(2)}u_4^{(3)} + u_1^{(3)}u_2^{(3)}u_3^{(3)}u_4^{(2)}) \\ &+ \begin{pmatrix} c_{41} \\ 0 \\ e_{41} \end{pmatrix} u_1^{(3)}u_2^{(3)}u_3^{(3)}u_4^{(3)}, \end{aligned}$$

$$\begin{aligned} E(u_1,u_2,u_3,u_4,u_5,\mu) = &\begin{pmatrix} 0 \\ 0 \\ e_{40} \end{pmatrix} (u_1^{(2)}u_2^{(3)}u_3^{(3)}u_4^{(3)}u_5^{(3)} + u_1^{(3)}u_2^{(2)}u_3^{(3)}u_4^{(3)}u_5^{(3)} + u_1^{(3)}u_2^{(3)}u_3^{(2)}u_4^{(3)}u_5^{(3)} \\ &+ u_1^{(3)}u_2^{(3)}u_3^{(3)}u_4^{(2)}u_5^{(3)} + u_1^{(3)}u_2^{(3)}u_3^{(3)}u_4^{(3)}u_5^{(2)}) + \begin{pmatrix} c_{41} \\ 0 \\ e_{41} \end{pmatrix} u_1^{(3)}u_2^{(3)}u_3^{(3)}u_4^{(3)}u_5^{(3)} \end{aligned}$$

and

$$e_{20} = -\frac{\upsilon_{\text{mel}}(g^*+u_2)}{(M_2+g^*+u_2)^2}, \quad c_{21} = -\frac{2\alpha_A b}{(M_2+b)^3}, \quad e_{21} = 2\left(\frac{\upsilon_{\text{mel}}T_2(g^*+u_2)}{(M_2+g^*+u_2)^3} - \frac{\gamma_{\text{mel}}}{k}\right),$$

$$e_{30} = \frac{2\upsilon_{\text{mel}}(g^*+u_2)}{(M_2+g^*+u_2)^3}, \quad c_{31} = \frac{6\alpha_A b}{(M_2+b)^4}, \quad e_{31} = -\frac{6\upsilon_{\text{mel}}T_2(g^*+u_2)}{(M_2+g^*+u_2)^4},$$

$$e_{40} = -\frac{6\upsilon_{\mathrm{mel}}(g^* + u_2)}{(M_2 + g^* + u_2)^4}, \quad c_{41} = -\frac{24\alpha_A b}{(M_2 + b)^5}, \quad e_{41} = \frac{24\upsilon_{\mathrm{mel}} T_2(g^* + u_2)}{(M_2 + g^* + u_2)^5},$$
$$e_{50} = \frac{24\upsilon_{\mathrm{mel}}(g^* + u_2)}{(M_2 + g^* + u_2)^5}, \quad c_{51} = \frac{120\alpha_A b}{(M_2 + b)^6}, \quad e_{51} = \frac{120\upsilon_{\mathrm{mel}} T_2(g^* + u_2)}{(M_2 + g^* + u_2)^6}.$$

Let $q(\mu)$ be the eigenvector corresponding to the eigenvalue $\lambda(\mu)$ of the matrix $J_{E_2}(\mu)$, and $p(\mu)$ be the eigenvector corresponding to the eigenvalue $\overline{\lambda}(\mu)$ of the matrix $J^T_{E_2}(\mu)$. In addition, $q(\mu)$ and $p(\mu)$ satisfy the following condition

$$\langle p(\mu), q(\mu)\rangle = \overline{p}_1(\mu)q_1(\mu) + \overline{p}_2(\mu)q_2(\mu) + \overline{p}_3(\mu)q_3(\mu) = 1.$$

Therefore, we have

$$q(\mu) = \left(1, \frac{\alpha_e^* + \mu_1}{\lambda(\mu) + \mu_e}, \frac{(\lambda(\mu) + \mu_A)(M_2 + b)^2}{\alpha_A b}\right)^T,$$
$$p(\mu) = \left(1, \frac{\lambda(\mu) + \mu_A}{\alpha_e^* + \mu_1}, -\frac{(\lambda(\mu) + \mu_A)(\lambda(\mu) + \mu_e)(M_2 + g^* + \mu_2)}{\upsilon_{\mathrm{mel}} M_2}\right)^T.$$

Finally, according to [Zhang & Niu, 2020], we can calculate the expression of $l_2(0)$

$$\begin{aligned} 12l_2(0) = {} & \frac{1}{\omega_0}\operatorname{Re} g_{32} + \frac{1}{\omega_0^2}\operatorname{Im}\left[g_{20}\overline{g}_{31} - g_{11}(4g_{31} + 3\overline{g}_{22}) - \frac{1}{3}g_{02}(g_{40} + \overline{g}_{13}) - g_{30}g_{12}\right] \\ & + \frac{1}{\omega_0^3}\operatorname{Re}\left[g_{20}\overline{g}_{11}(3g_{12} - \overline{g}_{30}) + g_{20}g_{02}\left(\overline{g}_{12} - \frac{1}{3}g_{30}\right) + \frac{1}{3}g_{20}\overline{g}_{02}g_{30} + g_{11}\overline{g}_{02}\left(\frac{5}{3}\overline{g}_{30} + 3g_{12}\right)\right] \\ & + \frac{1}{\omega_0^3}\operatorname{Re}\left[\frac{1}{3}g_{11}g_{02}\overline{g}_{03} - 4g_2^{11}g_{30}\right] + \frac{3}{\omega_0^3}\operatorname{Im}(g_{20}g_{11})\operatorname{Im} g_{21} + \frac{1}{\omega_0^4}\operatorname{Im}[g_{11}\overline{g}_{02}(\overline{g}_{20}^2 - 3\overline{g}_{20}g_{11} - 4g_{11}^2] \\ & + \frac{1}{\omega_0^4}\operatorname{Im}(g_{20}g_{11})[3\operatorname{Re}(g_{20}g_{11}) - 2|g_{02}|^2], \end{aligned}$$

in which

$$\begin{aligned} & g_{20} = \langle p, B(q, q, 0)\rangle, \quad g_{11} = \langle p, B(q, \overline{q}, 0)\rangle, \quad g_{21} = \langle p, C(q, \overline{q}, 0)\rangle, \\ & g_{02} = \langle p, B(\overline{q}, \overline{q}, 0)\rangle, \quad g_{30} = \langle p, C(q, q, q, 0)\rangle, \quad g_{12} = \langle p, C(q, \overline{q}, \overline{q}, 0)\rangle, \\ & g_{03} = \langle p, C(\overline{q}, \overline{q}, \overline{q}, 0)\rangle, \quad g_{40} = \langle p, D(q, q, q, q, 0)\rangle, \quad g_{31} = \langle p, D(q, q, q, \overline{q}, 0)\rangle, \\ & g_{22} = \langle p, D(q, q, \overline{q}, \overline{q}, 0)\rangle, \quad g_{13} = \langle p, D(q, \overline{q}, \overline{q}, \overline{q}, 0)\rangle, \quad g_{32} = \langle p, E(q, q, q, \overline{q}, \overline{q}, 0)\rangle. \end{aligned}$$

The first Lyapunov coefficient $l_1(\mu)$ is expressed as follows

$$l_1(\mu) = \frac{\operatorname{Re}[c_1(\mu)]}{\omega(\mu)} - \xi(\mu)\frac{\operatorname{Im}[c_1(\mu)]}{\omega^2(\mu)}, \tag{A.4}$$

where

$$c_1(\mu) = \frac{g_{21}(\mu)}{2} + \frac{|g_{11}(\mu)|^2}{\lambda(\mu)} + \frac{|g_{02}(\mu)|^2}{2(2\lambda(\mu) - \overline{\lambda}(\mu))} + \frac{g_{20}(\mu)g_{11}(\mu)(2\lambda(\mu) + \overline{\lambda}(\mu))}{2|\lambda(\mu)|^2}.$$

A.3. *Calculation of the normal form of Bogdanov–Takens bifurcation*

Let $\alpha_e = \alpha_e^{**}$ and $g = g^{**}$ be the bifurcation parameter values, η_1 and η_2 be the eigenvector and generalized eigenvector of eigenvalue λ_1, respectively, and η_3 be the eigenvector of eigenvalue λ_3. According to $J_{E_*^2}\eta_1 = \lambda_1\eta_1$, $J_{E_2^*}\eta_2 = \eta_1$ and $J_{E_2^*}\eta_3 = \lambda_3\eta_3$, we have

$$\eta_1 = \begin{pmatrix} \alpha_A \dfrac{b}{(M_2^* + b)^2} \\ 0 \\ \mu_A \end{pmatrix},$$

$$\eta_2 = \begin{pmatrix} \mu_e \\ \alpha_e \\ \dfrac{(M_2^* + b)^2\mu_A\mu_e + \alpha_e b}{\alpha_A b} \end{pmatrix},$$

$$\eta_3 = \begin{pmatrix} \alpha_A \dfrac{b}{(M_2^* + b)^2} \\ -\dfrac{\alpha_e\alpha_A b}{(\overline{\Delta}_1(E_2^*) - \mu_A)(M_2^* + b)^2} \\ \overline{\Delta}_1(E_2^*) - \mu_e \end{pmatrix}.$$

Denote

$$Q = (\eta_1, \eta_2, \eta_3) = \begin{pmatrix} \theta & \mu_e & \theta \\ 0 & \alpha_e & n \\ \mu_A & p & q \end{pmatrix},$$

where

$$\theta = \alpha_A \frac{b}{(M_2^* + b)^2},$$

$$n = -\frac{\alpha_e\alpha_A b}{(\overline{\Delta}_1(E_2^*) - \mu_A)(M_2^* + b)^2},$$

$$p = \frac{(M_2^* + b)^2\mu_A\mu_e + \alpha_e b}{\alpha_A b},$$

$$q = \overline{\Delta}_1(E_2^*) - \mu_e,$$

then

$$Q^{-1} = \begin{pmatrix} q_{11} & q_{12} & q_{13} \\ q_{21} & q_{22} & q_{23} \\ q_{31} & q_{32} & q_{33} \end{pmatrix},$$

where

$$q_{11} = \frac{-\alpha_e q + np}{\alpha_e\theta\mu_A - \alpha_e\theta q - \mu_A\mu_e n + \theta np},$$

$$q_{12} = \frac{-\theta p + \mu_e q}{\alpha_e\theta\mu_A - \alpha_e q\theta - \mu_A\mu_e n + \theta np},$$

$$q_{13} = \frac{\alpha_e\theta - \mu_e n}{\alpha_e\theta\mu_A - \alpha_e\theta q - \mu_A\mu_e n + \theta np},$$

$$q_{21} = \frac{-\mu_A n}{\alpha_e\theta\mu_A - \alpha_e\theta q - \mu_A\mu_e n + \theta np},$$

$$q_{22} = \frac{\theta\mu_A - \theta q}{\alpha_e\theta\mu_A - \alpha_e\theta q - \mu_A\mu_e n + \theta np},$$

$$q_{23} = \frac{\theta n}{\alpha_e\theta\mu_A - \alpha_e\theta q - \mu_A\mu_e n + \theta np},$$

$$q_{31} = \frac{\alpha_e\mu_A}{\alpha_e\theta\mu_A - \alpha_e\theta q - \mu_A\mu_e n + \theta np},$$

$$q_{32} = \frac{-\mu_A\mu_e + \theta p}{\alpha_e\theta\mu_A - \alpha_e\theta q - \mu_A\mu_e n + \theta np},$$

$$q_{33} = \frac{-\alpha_e\theta}{\alpha_e\theta\mu_A - \alpha_e\theta q - \mu_A\mu_e n + \theta np}.$$

Applying the following coordinates transformations to (2) to put the system in the standard form

$$\begin{pmatrix} x \\ y \\ z \end{pmatrix} = Q \begin{pmatrix} A \\ T \\ M \end{pmatrix},$$

which yields

$$\begin{pmatrix} \dfrac{\mathrm{d}x}{\mathrm{d}t} \\ \dfrac{\mathrm{d}y}{\mathrm{d}t} \\ \dfrac{\mathrm{d}z}{\mathrm{d}t} \end{pmatrix} = \begin{pmatrix} 0 & 1 & 0 \\ 0 & 0 & 0 \\ 0 & 0 & \overline{\Delta}_1(E_2^*) - (\mu_A + \mu_e) \end{pmatrix} \begin{pmatrix} x \\ y \\ z \end{pmatrix} + \begin{pmatrix} w_1 \\ w_2 \\ w_3 \end{pmatrix}, \tag{A.5}$$

where

$$w_1 = w_{11}x^2 + w_{12}xy + w_{13}xz + w_{14}yz + w_{15}y^2 + w_{16}z^2,$$

$$w_2 = w_{21}x^2 + w_{22}xy + w_{23}xz + w_{24}yz + w_{25}y^2 + w_{26}z^2,$$

$$w_3 = w_{31}x^2 + w_{32}xy + w_{33}xz + w_{34}yz + w_{35}y^2 + w_{36}z^2.$$

The coefficients of w_1, w_2 and w_3 are

$$\begin{aligned}
w_{11} &= \theta q_{31}^2(n_{11}+n_{13}) + \theta n_{12}q_{21}q_{31},\\
w_{12} &= 2\theta q_{31}q_{32}(n_{11}+n_{13}) + \theta n_{12}(q_{21}q_{32}+q_{22}q_{31}),\\
w_{13} &= 2\theta q_{31}q_{33}(n_{11}+n_{13}) + \theta n_{12}(q_{21}q_{33}+q_{23}q_{31}),\\
w_{14} &= 2\theta q_{32}q_{33}(n_{11}+n_{13}) + \theta n_{12}(q_{21}q_{33}+q_{23}q_{31}),\\
w_{15} &= \theta q_{32}^2(n_{11}+n_{13}) + \theta n_{11}q_{22}q_{32},\\
w_{16} &= \theta q_{33}^2(n_{11}+n_{13}) + \theta n_{11}q_{23}q_{33},\\
w_{21} &= nq_{31}^2n_{13} + nn_{12}q_{21}q_{31},\\
w_{22} &= 2nq_{31}q_{32}n_{13} + nn_{12}(q_{21}q_{32}+q_{22}q_{31}),\\
w_{23} &= 2nq_{31}q_{33}n_{13} + nn_{12}(q_{21}q_{33}+q_{23}q_{31}),\\
w_{24} &= 2nq_{32}q_{33}n_{13} + nn_{12}(q_{21}q_{33}+q_{23}q_{31}),\\
w_{25} &= nq_{32}^2n_{13} + nn_{11}q_{22}q_{32},\\
w_{26} &= nq_{33}^2n_{13} + nn_{11}q_{23}q_{33},\\
w_{31} &= q_{31}^2(\mu_A n_{11} + qn_{13}) + qn_{12}q_{21}q_{31},\\
w_{32} &= 2q_{31}q_{32}(\mu_A n_{11} + qn_{13}) + qn_{12}(q_{21}q_{32}+q_{22}q_{31}),\\
w_{33} &= 2q_{31}q_{33}(\mu_A n_{11} + qn_{13}) + qn_{12}(q_{21}q_{33}+q_{23}q_{31}),\\
w_{34} &= 2q_{32}q_{33}(\mu_A n_{11} + qn_{13}) + qn_{12}(q_{21}q_{33}+q_{23}q_{31}),\\
w_{35} &= q_{32}^2(\mu_A n_{11} + qn_{13}) + qn_{11}q_{22}q_{32},\\
w_{36} &= q_{33}^2(\mu_A n_{11} + qn_{13}) + qn_{11}q_{23}q_{33}.
\end{aligned}$$

Considering $z = h_1(x,y) = r_1x^2 + s_1xy + t_1y^2 + \text{h.o.t}$, we have

$$2r_1x\frac{\mathrm{d}x}{\mathrm{d}t} + s_1x\frac{\mathrm{d}y}{\mathrm{d}t} + s_1y\frac{\mathrm{d}x}{\mathrm{d}t} + 2t_1y\frac{\mathrm{d}y}{\mathrm{d}t} = [\overline{\Delta}_1(E_2^*) - (\mu_A+\mu_e)]z + w_3.$$

By comparing the coefficients of x^2, xy and y^2 on the left and right sides of the above formula, it can be concluded that

$$\begin{aligned}
&[\overline{\Delta}_1(E_2^*) - (\mu_A+\mu_e)]r_1 + w_{31} = 0,\\
&[\overline{\Delta}_1(E_2^*) - (\mu_A+\mu_e)]s_1 + w_{32} = 2r_1,\\
&[\overline{\Delta}_1(E_2^*) - (\mu_A+\mu_e)]t_1 + w_{35} = s_1
\end{aligned}$$

and

$$\begin{aligned}
r_1 &= -\frac{w_{31}}{\overline{\Delta}_1(E_2^*) - (\mu_A+\mu_e)},\\
s_1 &= -\frac{2w_{31}}{[\overline{\Delta}_1(E_2^*) - (\mu_A+\mu_e)]^2} - \frac{w_{32}}{\overline{\Delta}(E_2^*) - (\mu_A+\mu_e)},\\
t_1 &= -\frac{2w_{31}}{[\overline{\Delta}_1(E_2^*) - (\mu_A+\mu_e)]^3} - \frac{w_{32}}{[\overline{\Delta}_1(E_2^*) - (\mu_A+\mu_e)]^2} - \frac{w_{35}}{\overline{\Delta}_1(E_2^*) - (\mu_A+\mu_e)}.
\end{aligned}$$

Thus, the dynamics of the system (A.5) restricted to the center manifold is determined by

$$\begin{pmatrix} \dfrac{\mathrm{d}x}{\mathrm{d}t} \\ \dfrac{\mathrm{d}y}{\mathrm{d}t} \end{pmatrix} = \begin{pmatrix} 0 & 1 \\ 0 & 0 \end{pmatrix} \begin{pmatrix} x \\ y \end{pmatrix} + \begin{pmatrix} W_1 \\ W_2 \end{pmatrix}, \tag{A.6}$$

where

$$\begin{aligned}
W_1 &= w_{11}x^2 + w_{12}xy + w_{15}y^2 + (s_1w_{13} + r_1w_{14})x^2y + (t_1w_{13} + s_1w_{14})xy^2 + r_1w_{13}x^3 + t_1w_{14}y^3,\\
W_2 &= w_{21}x^2 + w_{22}xy + w_{25}y^2 + (s_1w_{23} + r_1w_{24})x^2y + (t_1w_{23} + s_1w_{24})xy^2 + r_1w_{23}x^3 + t_1w_{24}y^3.
\end{aligned}$$

Conditional normal form at bifurcation values of parameters can be obtained by using the following transformation

$$\begin{cases} u_1 = x, \\ u_2 = y + W_1. \end{cases}$$

The normal form of the original system at the equilibrium point E_2^* is obtained

$$\begin{cases} \dfrac{\mathrm{d}u_1}{\mathrm{d}t} = u_2, \\ \dfrac{\mathrm{d}u_2}{\mathrm{d}t} = w_{11}u_1^2 + (2w_{11} + w_{22})u_1u_2 \\ \qquad\qquad + (w_{25} + w_{11})u_2^2 + O(|(u_1, u_2)|^3). \end{cases} \tag{A.7}$$

Up to now, we calculate the universal folding of Bogdanov–Takens bifurcation by adding a disturbance to the bifurcation parameter, namely $g = g^{**} + \varepsilon_1$, $\alpha_e = \alpha_e^{**} + \varepsilon_2$. Using the same method as before, we have

$$\begin{pmatrix} \dfrac{\mathrm{d}x}{\mathrm{d}t} \\ \dfrac{\mathrm{d}y}{\mathrm{d}t} \\ \dfrac{\mathrm{d}z}{\mathrm{d}t} \end{pmatrix} = \begin{pmatrix} 0 & 1 & 0 \\ 0 & 0 & 0 \\ 0 & 0 & \overline{\Delta}_1(E_2^*) - (\mu_A + \mu_e) \end{pmatrix} \begin{pmatrix} x \\ y \\ z \end{pmatrix} + \begin{pmatrix} w_1'(x, y, z, \varepsilon_1, \varepsilon_2) \\ w_2'(x, y, z, \varepsilon_1, \varepsilon_2) \\ w_3'(x, y, z, \varepsilon_1, \varepsilon_2) \end{pmatrix}, \tag{A.8}$$

in which

$$\begin{aligned} &w_1'(x, y, z, \varepsilon_1, \varepsilon_2) \\ &\quad = w_{11}'(\varepsilon_1, \varepsilon_2)x^2 + w_{12}'(\varepsilon_1, \varepsilon_2)xy \\ &\qquad + w_{13}'(\varepsilon_1, \varepsilon_2)xz + w_{14}'(\varepsilon_1, \varepsilon_2)yz \\ &\qquad + w_{15}'(\varepsilon_1, \varepsilon_2)y^2 + w_{16}'(\varepsilon_1, \varepsilon_2)z^2, \\ &w_2'(x, y, z, \varepsilon_1, \varepsilon_2) \\ &\quad = w_{21}'(\varepsilon_1, \varepsilon_2)x^2 + w_{22}'(\varepsilon_1, \varepsilon_2)xy \\ &\qquad + w_{23}'(\varepsilon_1, \varepsilon_2)xz + w_{24}'(\varepsilon_1, \varepsilon_2)yz \\ &\qquad + w_{25}'(\varepsilon_1, \varepsilon_2)y^2 + w_{26}'(\varepsilon_1, \varepsilon_2)z^2, \\ &w_3'(x, y, z, \varepsilon_1, \varepsilon_2) \\ &\quad = w_{31}'(\varepsilon_1, \varepsilon_2)x^2 + w_{32}'(\varepsilon_1, \varepsilon_2)xy \\ &\qquad + w_{33}'(\varepsilon_1, \varepsilon_2)xz + w_{34}'(\varepsilon_1, \varepsilon_2)yz \\ &\qquad + w_{35}'(\varepsilon_1, \varepsilon_2)y^2 + w_{36}'(\varepsilon_1, \varepsilon_2)z^2 \end{aligned}$$

and

$$\begin{aligned} w_{11}'(\varepsilon_1, \varepsilon_2) &= \theta(q_{31}')^2(n_{11} + n_{13}) + \theta n_{12}q_{21}'q_{31}', \\ w_{12}'(\varepsilon_1, \varepsilon_2) &= 2\theta q_{31}'q_{32}'(n_{11} + n_{13}) \\ &\quad + \theta n_{12}(q_{21}'q_{32}' + q_{22}'q_{31}'), \\ w_{13}'(\varepsilon_1, \varepsilon_2) &= 2\theta q_{31}'q_{33}'(n_{11} + n_{13}) \\ &\quad + \theta n_{12}(q_{21}'q_{33}' + q_{23}'q_{31}'), \\ w_{14}'(\varepsilon_1, \varepsilon_2) &= 2\theta q_{32}'q_{33}'(n_{11} + n_{13}) \\ &\quad + \theta n_{12}(q_{21}'q_{33}' + q_{23}'q_{31}'), \\ w_{15}'(\varepsilon_1, \varepsilon_2) &= \theta(q_{32}')^2(n_{11} + n_{13}) + \theta n_{11}q_{22}'q_{32}', \\ w_{16}'(\varepsilon_1, \varepsilon_2) &= \theta(q_{33}')^2(n_{11} + n_{13}) + \theta n_{11}q_{23}'q_{33}', \\ w_{21}'(\varepsilon_1, \varepsilon_2) &= n'(q_{31}')^2n_{13} + n'n_{12}q_{21}'q_{31}', \\ w_{22}'(\varepsilon_1, \varepsilon_2) &= 2n'q_{31}'q_{32}'n_{13} + n'n_{12}(q_{21}'q_{32}' + q_{22}'q_{31}'), \\ w_{23}'(\varepsilon_1, \varepsilon_2) &= 2n'q_{31}'q_{33}'n_{13} + n'n_{12}(q_{21}'q_{33}' + q_{23}'q_{31}'), \\ w_{24}'(\varepsilon_1, \varepsilon_2) &= 2n'q_{33}'q_{32}'n_{13} + n'n_{12}(q_{21}'q_{33}' + q_{23}'q_{31}'), \\ w_{25}'(\varepsilon_1, \varepsilon_2) &= n'(q_{32}')^2n_{13} + n'n_{12}q_{22}'q_{32}', \\ w_{26}'(\varepsilon_1, \varepsilon_2) &= n'(q_{33}')^2n_{13} + n'n_{12}q_{23}'q_{33}', \\ w_{31}'(\varepsilon_1, \varepsilon_2) &= (q_{31}')^2(\mu_An_{11} + q'n_{13}) + q'n_{12}q_{21}'q_{31}', \\ w_{32}'(\varepsilon_1, \varepsilon_2) &= 2q_{31}'q_{32}'(\mu_An_{11} + q'n_{13}) \\ &\quad + q'n_{12}(q_{21}'q_{32}' + q_{22}'q_{31}'), \\ w_{33}'(\varepsilon_1, \varepsilon_2) &= 2q_{31}'q_{33}'(\mu_An_{11} + q'n_{13}) \\ &\quad + q'n_{12}(q_{21}'q_{33}' + q_{23}'q_{31}'), \\ w_{34}'(\varepsilon_1, \varepsilon_2) &= 2q_{33}'q_{32}'(\mu_An_{11} + q'n_{13}) \\ &\quad + q'n_{12}(q_{21}'q_{33}' + q_{23}'q_{31}'), \\ w_{35}'(\varepsilon_1, \varepsilon_2) &= (q_{32}')^2(\mu_An_{11} + q'n_{13}) + q'n_{12}q_{22}'q_{32}', \\ w_{36}'(\varepsilon_1, \varepsilon_2) &= (q_{33}')^2(\mu_An_{11} + q'n_{13}) + q'n_{12}q_{23}'q_{33}' \end{aligned}$$

and

$$\begin{aligned} \theta &= \alpha_A\frac{b}{(M_2^* + b)^2}, \\ n' &= -\frac{(\alpha_e^* + \varepsilon_2)\alpha_Ab}{(\overline{\Delta}_1(E_2^*) - \mu_A)(M_2^* + b)^2}, \\ p' &= \frac{(M_2^* + b)^2\mu_e - (\alpha_e^* + \varepsilon_2)b}{\alpha_Ab}, \\ q' &= \overline{\Delta}_1(E_2^*) - \mu_e \end{aligned}$$

and

$$q'_{11}(\varepsilon_1,\varepsilon_2)=\frac{-(\alpha_e^{**}+\varepsilon_2)q'+n'p'}{(\alpha_e^{**}+\varepsilon_2)\theta\mu_A-(\alpha_e^{**}+\varepsilon_2)\theta q'-\mu_A\mu_e n+\theta n'p'},$$

$$q'_{21}(\varepsilon_1,\varepsilon_2)=\frac{-\theta p'+\mu_e q'}{(\alpha_e^{**}+\varepsilon_2)\theta\mu_A-(\alpha_e^{**}+\varepsilon_2)\theta q'-\mu_A(\alpha_e^{**}+\varepsilon_2)n+\theta n'p'},$$

$$q'_{31}(\varepsilon_1,\varepsilon_2)=\frac{(\alpha_e^{**}+\varepsilon_2)\theta-\mu_e n'}{(\alpha_e^{**}+\varepsilon_2)\theta\mu_A-(\alpha_e^{**}+\varepsilon_2)\theta q'-\mu_A(\alpha_e^{**}+\varepsilon_2)n+\theta n'p'},$$

$$q'_{21}(\varepsilon_1,\varepsilon_2)=\frac{\alpha_A n'}{(\alpha_e^{**}+\varepsilon_2)\theta\mu_A-(\alpha_e^{**}+\varepsilon_2)\theta q'-\mu_A(\alpha_e^{**}+\varepsilon_2)n+\theta n'p'},$$

$$q'_{22}(\varepsilon_1,\varepsilon_2)=\frac{\theta\alpha_A-\theta q'}{(\alpha_e^{**}+\varepsilon_2)\theta\mu_A-(\alpha_e^{**}+\varepsilon_2)\theta q'-\mu_A(\alpha_e^{**}+\varepsilon_2)n+\theta n'p'},$$

$$q'_{23}(\varepsilon_1,\varepsilon_2)=\frac{\theta n'}{(\alpha_e^{**}+\varepsilon_2)\theta\mu_A-(\alpha_e^{**}+\varepsilon_2)\theta q'-\mu_A(\alpha_e^{**}+\varepsilon_2)n+\theta n'p'},$$

$$q'_{31}(\varepsilon_1,\varepsilon_2)=\frac{(\alpha_e^{**}+\varepsilon_2)\mu_A}{(\alpha_e^{**}+\varepsilon_2)\theta\mu_A-(\alpha_e^{**}+\varepsilon_2)\theta q'-\mu_A\mu_e n+\theta n'p'},$$

$$q'_{32}(\varepsilon_1,\varepsilon_2)=\frac{-\mu_e\mu_A+\theta p'}{(\alpha_e^{**}+\varepsilon_2)\theta\mu_A-(\alpha_e^{**}+\varepsilon_2)\theta q'-\mu_A(\alpha_e^{**}+\varepsilon_2)n+\theta n'p'},$$

$$q'_{33}(\varepsilon_1,\varepsilon_2)=\frac{-(\alpha_e^{**}+\varepsilon_2)\theta}{(\alpha_e^{**}+\varepsilon_2)\theta\mu_A-(\alpha_e^{**}+\varepsilon_2)\theta q'-\mu_A(\alpha_e^{**}+\varepsilon_2)n+\theta n'p'}.$$

There is the following center manifold dependent parameter

$$[\overline{\Delta}_1-(\mu_A+\mu_e)]\sum_{\substack{i+j+k+l\geq 2\\ i,j,k,l=0}}^{3}a_{ijkl}x^iy^j\varepsilon_1^k\varepsilon_2^l+w'_3(x,y,z,\varepsilon_1,\varepsilon_2)=\frac{\mathrm{d}}{\mathrm{d}t}\left[\sum_{\substack{i+j+k+l\geq 2\\ i,j,k,l=0}}^{3}a_{ijkl}x^iy^j\varepsilon_1^k\varepsilon_2^l\right].$$

So system (A.8) can be reduced to

$$\begin{pmatrix}\dot{x}\\ \dot{y}\end{pmatrix}=\begin{pmatrix}0 & 1\\ 0 & 0\end{pmatrix}\begin{pmatrix}x\\ y\end{pmatrix}+\begin{pmatrix}G_1(x,y,\varepsilon_1,\varepsilon_2)\\ G_2(x,y,\varepsilon_1,\varepsilon_2)\end{pmatrix},$$

where

$$\begin{aligned}&G_1(x,y,\varepsilon_1,\varepsilon_2)\\ &=w'_{11}(\varepsilon_1,\varepsilon_2)x^2+w'_{12}(\varepsilon_1,\varepsilon_2)xy+w'_{13}(\varepsilon_1,\varepsilon_2)x\sum_{\substack{i+j+k+l\geq 2\\ i,j,k,l=0}}^{3}a_{ijkl}x^iy^j\varepsilon_1^k\varepsilon_2^l\\ &\quad+w'_{14}(\varepsilon_1,\varepsilon_2)y\sum_{\substack{i+j+k+l\geq 2\\ i,j,k,l=0}}^{3}a_{ijkl}x^iy^j\varepsilon_1^k\varepsilon_2^l+w'_{15}(\varepsilon_1,\varepsilon_2)y^2+w'_{16}(\varepsilon_1,\varepsilon_2)\left[\sum_{\substack{i+j+k+l\geq 2\\ i,j,k,l=0}}^{3}a_{ijkl}x^iy^j\varepsilon_1^k\varepsilon_2^l\right]^2,\end{aligned}$$

$$
\begin{aligned}
&G_2(x,y,z,\varepsilon_1,\varepsilon_2)\\
&\quad= w'_{21}(\varepsilon_1,\varepsilon_2)x^2 + w'_{22}(\varepsilon_1,\varepsilon_2)xy + w'_{23}(\varepsilon_1,\varepsilon_2)x \sum_{\substack{i+j+k+l\geq 2\\ i,j,k,l=0}}^{3} a_{ijkl}x^i y^j \varepsilon_1^k \varepsilon_2^l\\
&\quad\quad + w'_{24}(\varepsilon_1,\varepsilon_2)y \sum_{\substack{i+j+k+l\geq 2\\ i,j,k,l=0}}^{3} a_{ijkl}x^i y^j \varepsilon_1^k \varepsilon_2^l + w'_{25}(\varepsilon_1,\varepsilon_2)y^2 + w'_{26}(\varepsilon_1,\varepsilon_2)\left[\sum_{\substack{i+j+k+l\geq 2\\ i,j,k,l=0}}^{3} a_{ijkl}x^i y^j \varepsilon_1^k \varepsilon_2^l\right]^2.
\end{aligned}
$$

According to reference [Peng & Li, 2014], it is calculated that

$$
\begin{aligned}
c_{30} &= -\frac{p_{10}^4 p_{30}}{p_{01}^3} + \frac{p_{10}^3(p_{12}-q_{03})}{p_{01}^2} - \frac{p_{10}^2(p_{21}-q_{12})}{p_{01}} - p_{01}p_{30} - p_{10}q_{21} + p_{01}q_{30},\\
c_{21} &= \frac{p_{10}^2(p_{12}+3q_{03})}{p_{01}^2} - \frac{2p_{10}(p_{21}+q_{12})}{p_{01}} + 3p_{30} + q_{21},
\end{aligned}
$$

here

$$
\begin{aligned}
p_{01} &= (w'_{14}(\varepsilon_1,\varepsilon_2) + w'_{16}(\varepsilon_1,\varepsilon_2)(a_{0110}\varepsilon_1 + a_{0101}\varepsilon_2 + a_{0120}\varepsilon_1^2 + a_{0102}\varepsilon_2^2))\\
&\quad\times(a_{0011}\varepsilon_1\varepsilon_2 + a_{0020}\varepsilon_1^2 + a_{0002}\varepsilon_2^2 + a_{0021}\varepsilon_1^2\varepsilon_2 + a_{0012}\varepsilon_1\varepsilon_2^2 + a_{0030}\varepsilon_1^3 + a_{0003}\varepsilon_2^3),\\
p_{10} &= (w'_{13}(\varepsilon_1,\varepsilon_2) + w'_{16}(\varepsilon_1,\varepsilon_2)(a_{1001}\varepsilon_2 + a_{1010}\varepsilon_1 + a_{1020}\varepsilon_1^2 + a_{1002}\varepsilon_2^2))\\
&\quad\times(a_{0011}\varepsilon_1\varepsilon_2 + a_{0020}\varepsilon_1^2 + a_{0002}\varepsilon_2^2 + a_{0021}\varepsilon_1^2\varepsilon_2 + a_{0012}\varepsilon_1\varepsilon_2^2 + a_{0030}\varepsilon_1^3 + a_{0003}\varepsilon_2^3),\\
p_{12} &= \frac{1}{2}w'_{13}(\varepsilon_1,\varepsilon_2)(a_{1100} + a_{1110}\varepsilon_1 + a_{1101}\varepsilon_2) + \frac{1}{2}w'_{14}(\varepsilon_1,\varepsilon_2)(a_{2000} + a_{2010}\varepsilon_1 + a_{2001}\varepsilon_2) + \frac{1}{2}w'_{16}(\varepsilon_1,\varepsilon_2)\\
&\quad\times(a_{1100} + a_{1110}\varepsilon_1 + a_{1101}\varepsilon_2)(a_{1001}\varepsilon_2 + a_{1010}\varepsilon_1 + a_{1002}\varepsilon_2^2 + a_{1020}\varepsilon_1^2) + \frac{1}{2}w'_{16}(\varepsilon_1,\varepsilon_2)\\
&\quad\times(a_{2000} + a_{2001}\varepsilon_2 + a_{2010}\varepsilon_1)(a_{0110}\varepsilon_1 + a_{0111}\varepsilon_2 + a_{0201}\varepsilon_2^2 + a_{0120}\varepsilon_1^2) + \frac{1}{2}w'_{16}(\varepsilon_1,\varepsilon_2)a_{2100}\\
&\quad\times(a_{0011}\varepsilon_1\varepsilon_2 + a_{0020}\varepsilon_1^2 + a_{0002}\varepsilon_2^2 + a_{0021}\varepsilon_1^2\varepsilon_2 + a_{0012}\varepsilon_1\varepsilon_2^2 + a_{0030}\varepsilon_1^3 + a_{0003}\varepsilon_2^3),\\
p_{21} &= \frac{1}{2}w'_{13}(\varepsilon_1,\varepsilon_2)(a_{0200} + a_{0210}\varepsilon_1 + a_{0201}\varepsilon_2) + \frac{1}{2}w'_{14}(\varepsilon_1,\varepsilon_2)(a_{1100} + a_{1101}\varepsilon_1 + a_{1110}\varepsilon_2) + \frac{1}{2}w'_{16}(\varepsilon_1,\varepsilon_2)\\
&\quad\times(a_{1100} + a_{1110}\varepsilon_1 + a_{1101}\varepsilon_2)(a_{0101}\varepsilon_2 + a_{0110}\varepsilon_1 + a_{0102}\varepsilon_2^2 + a_{0120}\varepsilon_1^2) + \frac{1}{2}w'_{16}(\varepsilon_1,\varepsilon_2)\\
&\quad\times(a_{0200} + a_{0201}\varepsilon_2 + a_{0210}\varepsilon_1)(a_{1010}\varepsilon_1 + a_{1001}\varepsilon_2 + a_{1002}\varepsilon_2^2 + a_{1020}\varepsilon_1^2) + \frac{1}{2}w'_{16}(\varepsilon_1,\varepsilon_2)a_{1200}\\
&\quad\times(a_{0011}\varepsilon_1\varepsilon_2 + a_{0020}\varepsilon_1^2 + a_{0002}\varepsilon_2^2 + a_{0021}\varepsilon_1^2\varepsilon_2 + a_{0012}\varepsilon_1\varepsilon_2^2 + a_{0030}\varepsilon_1^3 + a_{0003}\varepsilon_2^3),\\
p_{03} &= \frac{1}{6}w'_{14}(\varepsilon_1,\varepsilon_2)(a_{0200} + a_{0210}\varepsilon_1 + a_{0201}\varepsilon_2) + \frac{1}{6}w'_{16}(\varepsilon_1,\varepsilon_2)a_{0300}\\
&\quad\times(a_{0011}\varepsilon_1\varepsilon_2 + a_{0020}\varepsilon_1^2 + a_{0002}\varepsilon_2^2 + a_{0021}\varepsilon_1^2\varepsilon_2 + a_{0012}\varepsilon_1\varepsilon_2^2 + a_{0030}\varepsilon_1^3 + a_{0003}\varepsilon_2^3)\\
&\quad + \frac{1}{6}w'_{16}(\varepsilon_1,\varepsilon_2)(a_{0101}\varepsilon_2 + a_{0110}\varepsilon_1 + a_{0111}\varepsilon_1\varepsilon_2)(a_{0200} + a_{0210}\varepsilon_1 + a_{0201}\varepsilon_2),
\end{aligned}
$$

$$
\begin{aligned}
q_{12} &= \frac{1}{2}w'_{23}(\varepsilon_1,\varepsilon_2)(a_{1100}+a_{1110}\varepsilon_1+a_{1101}\varepsilon_2)+\frac{1}{2}w'_{24}(\varepsilon_1,\varepsilon_2)(a_{2000}+a_{2010}\varepsilon_1+a_{2001}\varepsilon_2)+\frac{1}{2}w'_{26}(\varepsilon_1,\varepsilon_2)\\
&\quad\times(a_{1100}+a_{1110}\varepsilon_1+a_{1101}\varepsilon_2)(a_{1001}\varepsilon_2+a_{1010}\varepsilon_1+a_{1002}\varepsilon_2^2+a_{1020}\varepsilon_1^2)+\frac{1}{2}w'_{26}(\varepsilon_1,\varepsilon_2)\\
&\quad\times(a_{2000}+a_{2001}\varepsilon_2+a_{2010}\varepsilon_1)(a_{0110}\varepsilon_1+a_{0111}\varepsilon_2+a_{0201}\varepsilon_2^2+a_{0120}\varepsilon_1^2)+\frac{1}{2}w'_{26}(\varepsilon_1,\varepsilon_2)a_{2100}\\
&\quad\times(a_{0011}\varepsilon_1\varepsilon_2+a_{0020}\varepsilon_1^2+a_{0002}\varepsilon_2^2+a_{0021}\varepsilon_1^2\varepsilon_2+a_{0012}\varepsilon_1\varepsilon_2^2+a_{0030}\varepsilon_1^3+a_{0003}\varepsilon_2^3),\\
q_{21} &= \frac{1}{2}w'_{23}(\varepsilon_1,\varepsilon_2)(a_{0200}+a_{0210}\varepsilon_1+a_{0201}\varepsilon_2)+w'_{24}(\varepsilon_1,\varepsilon_2)(a_{1100}+a_{1101}\varepsilon_1+a_{1110}\varepsilon_2)+\frac{1}{2}w'_{26}(\varepsilon_1,\varepsilon_2)\\
&\quad\times(a_{1100}+a_{1110}\varepsilon_1+a_{1101}\varepsilon_2)(a_{0101}\varepsilon_2+a_{0110}\varepsilon_1+a_{0102}\varepsilon_2^2+a_{0120}\varepsilon_1^2)+\frac{1}{2}w'_{26}(\varepsilon_1,\varepsilon_2)\\
&\quad\times(a_{0200}+a_{0201}\varepsilon_2+a_{0210}\varepsilon_1)(a_{1010}\varepsilon_1+a_{1001}\varepsilon_2+a_{1002}\varepsilon_2^2+a_{1020}\varepsilon_1^2)+\frac{1}{2}w'_{26}(\varepsilon_1,\varepsilon_2)a_{1200}\\
&\quad\times(a_{0011}\varepsilon_1\varepsilon_2+a_{0020}\varepsilon_1^2+a_{0002}\varepsilon_2^2+a_{0021}\varepsilon_1^2\varepsilon_2+a_{0012}\varepsilon_1\varepsilon_2^2+a_{0030}\varepsilon_1^3+a_{0003}\varepsilon_2^3),\\
q_{03} &= \frac{1}{6}w'_{24}(\varepsilon_1,\varepsilon_2)(a_{0200}+a_{0210}\varepsilon_1+a_{0201}\varepsilon_2)+\frac{1}{6}w'_{26}(\varepsilon_1,\varepsilon_2)a_{0300}\\
&\quad\times(a_{0011}\varepsilon_1\varepsilon_2+a_{0020}\varepsilon_1^2+a_{0002}\varepsilon_2^2+a_{0021}\varepsilon_1^2\varepsilon_2+a_{0012}\varepsilon_1\varepsilon_2^2+a_{0030}\varepsilon_1^3+a_{0003}\varepsilon_2^3)\\
&\quad+\frac{1}{6}w'_{26}(\varepsilon_1,\varepsilon_2)(a_{0101}\varepsilon_2+a_{0110}\varepsilon_1+a_{0111}\varepsilon_1\varepsilon_2)(a_{0200}+a_{0210}\varepsilon_1+a_{0201}\varepsilon_2).
\end{aligned}
$$

Further calculation shows that

$$
\begin{aligned}
&\Delta_{01}=p_{01}|_{(\alpha_e,g)}-p_{01}|_{(\alpha_e,g)=(\alpha_e^{**}+\varepsilon_2,g^{**}+\varepsilon_1)},\quad \Delta_{10}=p_{10}|_{(\alpha_e,g)}-p_{10}|_{(\alpha_e,g)=(\alpha_e^{**}+\varepsilon_2,g^{**}+\varepsilon_1)},\\
&\delta_{01}=q_{01}|_{(\alpha_e,g)}-q_{01}|_{(\alpha_e,g)=(\alpha_e^{**}+\varepsilon_2,g^{**}+\varepsilon_1)},\quad \delta_{10}=q_{10}|_{(\alpha_e,g)}-q_{10}|_{(\alpha_e,g)=(\alpha_e^{**}+\varepsilon_2,g^{**}+\varepsilon_1)}.
\end{aligned}
$$

Therefore, we have

$$
\begin{aligned}
\phi_1(\varepsilon_1,\varepsilon_2)&=\frac{1}{c_{30}}\left[-\frac{\delta_{01}\delta_{10}(\Delta_{10}+\delta_{01})}{q_{10}}-\Delta_{10}\delta_{01}+\Delta_{01}(q_{10}+\delta_{10})\right],\\
\phi_2(\varepsilon_1,\varepsilon_2)&=\frac{1}{\sqrt{|c_{30}|}}\left[\frac{\delta_{10}^2(\Delta_{10}+\delta_{01})}{q_{10}^2}+\Delta_{10}+\delta_{01}\right].
\end{aligned}
$$

Finally, the universal unfolding of Bogdanov–Takens bifurcation is written as

$$
\begin{cases}
\dfrac{\mathrm{d}u_1}{\mathrm{d}t}=u_2,\\
\dfrac{\mathrm{d}u_2}{\mathrm{d}t}=\phi_1(\varepsilon_1,\varepsilon_2)u_1+\phi_2(\varepsilon_1,\varepsilon_2)u_2+w_{11}u_1^2+(2w_{11}+w_{22})u_1u_2+(w_{25}+w_{11})u_2^2.
\end{cases}
\tag{A.9}
$$

Furthermore, we take $w_{25}=-w_{11}$ to eliminate the u_2^2 term

$$
\begin{cases}
\dot{u}_1=u_2,\\
\dot{u}_2=\tilde{\phi}_1(\varepsilon_1,\varepsilon_2)u_1+\tilde{\phi}_2(\varepsilon_1,\varepsilon_2)u_2+\tilde{w}_{11}u_1^2+su_1u_2,
\end{cases}
\tag{A.10}
$$

where

$$
s=\mathrm{sign}(2w_{11}+w_{22})=\pm 1.
$$